Mémoire

Auteur : Reuter, Ylenia
Promoteur(s) : Grégoire, Marilaure; Choblet, Mathurin
Faculté : Faculté des Sciences
Diplôme : Master en océanographie, à finalité approfondie
Année académique : 2024-2025
URI/URL : http://hdl.handle.net/2268.2/23921

Author : Ylenia REUTER

Lagrangian modeling of microplastic fate and transport in the Black Sea

Under the Supervision of Marilaure GRÉGOIRE

A Thesis Submitted in Partial Fulfillment of the Requirements for the Master's Degree in Oceanography

University of Liege - Faculty of Sciences

Academic year 2024-2025

Supervising assistant : Mathurin CHOBLET

Jury members: Marilaure GRÉGOIRE, Krishna DAS, Jean-Marie BECKERS and Bruno FREDERICH

Conformément aux règles imposées à la rédaction, ce mémoire ne doit pas dépasser 50 pages, rédigées en Times 12 ou équivalent.

Table of contents

Acknowledgments

Firstly, I would like to thank Marilaure Grégoire for supervising my thesis project. She was a great help in setting appropriate goals and writing the objectives for this thesis. I thank her for her encouragement and for giving me the courage to try writing a thesis, despite my lack of coding experience.

I would also like to express my sincere gratitude to Mathurin Choblet for his patience during my novice learning process in coding and modelling. From the Canary Islands, where I had to install and create my credentials on Lucia, to the smallest changes I had to make to my plots at the last minute. Thank you also for questioning the results and for pushing me to always better understand my results.

I would like to warmly thank the MAST members, who took the time to go through my code and explain how these small elements that change everything in a code work. Without them, understanding and progressing in writing the simulations would not have been possible.

Finally, I would like to thank the members of the jury for their reading and support.

Abstract (VF et ENG)

[EN] Every year, 14 million tons of plastic reach the ocean, where they threaten ecosystems and human health. The Black Sea, a semi-enclosed basin with strong riverine inputs, offers a unique setting to investigate microplastic transport. Using the NEMO-BAMBHI model and Lagrangian simulations, we explored four scenarios: homogeneous releases (2D and 3D with sinking) and riverine releases with different sinking velocities. In the 2D simulation, accumulation hotspots appear along the southwestern coast, with particles largely following the Rim Current. Adding sinking (3D) significantly alters dispersion: particles display clustered trajectories, reduced beaching, and oscillations likely linked to vertical dynamics. Riverine scenarios reveal strong local retention near river mouths. Across all cases, accumulation consistently overlaps with ecologically sensitive areas such as the northwestern shelf and the Turkish coast. Sinking strongly reduces lateral transport, riverine inputs dominate accumulation patterns, and vulnerable coastal regions remain key hotspots. Continued investigation of vertical processes is essential to refine predictions of microplastic fate in enclosed seas.

[FR] Chaque année, 14 millions de tonnes de plastique atteignent les océans, où ils menacent les écosystèmes et la santé humaine. La mer Noire, un bassin semi-fermé avec d'importants apports fluviaux, offre un cadre unique pour étudier le transport des microplastiques. Avec le modèle NEMO-BAMBHI et des simulations lagrangiennes, nous avons exploré quatre scénarios : dispersions homogènes (en 2D et 3D, avec vitesse de sédimentation) et des lancements de particules depuis les différentes embouchures des rivières avec deux vitesses de sédimentation différentes. Dans la simulation 2D, des points d'accumulation apparaissent le long de la côte sud-ouest, les particules suivant en grande partie le courant principal de la mer Noire. L'ajout d'une vitesse (3D) modifie considérablement la dispersion : les particules présentent des trajectoires agglutinées, l'échouage diminue et l'on observe des oscillations probablement liées à la dynamique verticale. Les scénarios fluviaux révèlent une forte rétention locale près des embouchures des fleuves. Dans tous les cas, l'accumulation chevauche systématiquement des zones écologiquement sensibles telles que le plateau nord-ouest et la côte turque. La sédimentation réduit fortement le transport latéral, les apports fluviaux dominent les schémas d'accumulation et les régions côtières vulnérables restent des points chauds clés. La poursuite des recherches sur les processus verticaux est essentielle pour affiner les prévisions concernant les trajectoires du microplastique en mer Noire.

Introduction

The Black Sea

1. Generalities

The Black Sea is a semi-enclosed sea with an area of approximately 4.2×10^5 km². It extends between 40°55‘ and 46°32’ North latitude and 27°27‘ and 41°32’ East longitude, bordered by several countries including Romania, Bulgaria, Turkey, Georgia, Russia and Ukraine. This strategic geographical position makes it a complex area of hydrological exchange, influenced by massive river inflows, exchanges with other marine basins and a particular circulation dynamic. This sea is linked to other marine basins by two passages : the Bosphorus Strait, which connects it to the Sea of Marmara and, by extension, to the Mediterranean Sea via the Dardanelles Strait and, to the east, the Kerch Strait, which connects it to the Sea of Azov.

2. Circulations dynamics

The circulation dynamics of the Black Sea are dominated by two main cyclonic gyres, located in the western and eastern basins respectively. These gyres are fed by the Rim Current, a rapid circulation that runs along the margins of the continental shelf, created by the wind and coriolis forces, which are dominant in the Black Sea (Stanev, 2005). The Rim Current follows the continental slope on the northwestern and western side since the dynamics of the Black Sea is governed by the topography of the basin, the river inputs and meteorological conditions. In winter, the circulation intensifies, and horizontal transport can nearly double (Stanev, 2005), whereas in summer, the formation of sub-basin scale eddies becomes apparent. During this season, the thermohaline circulation is mainly controlled by salinity (Oguz et al., 1999; Stanev, 2005). The cyclonic circulation is enhanced by the haline buoyancy anomalies that stratifies the semi-enclosed basin because of the inputs of freshwater in the coastal areas (Stanev, 2005).

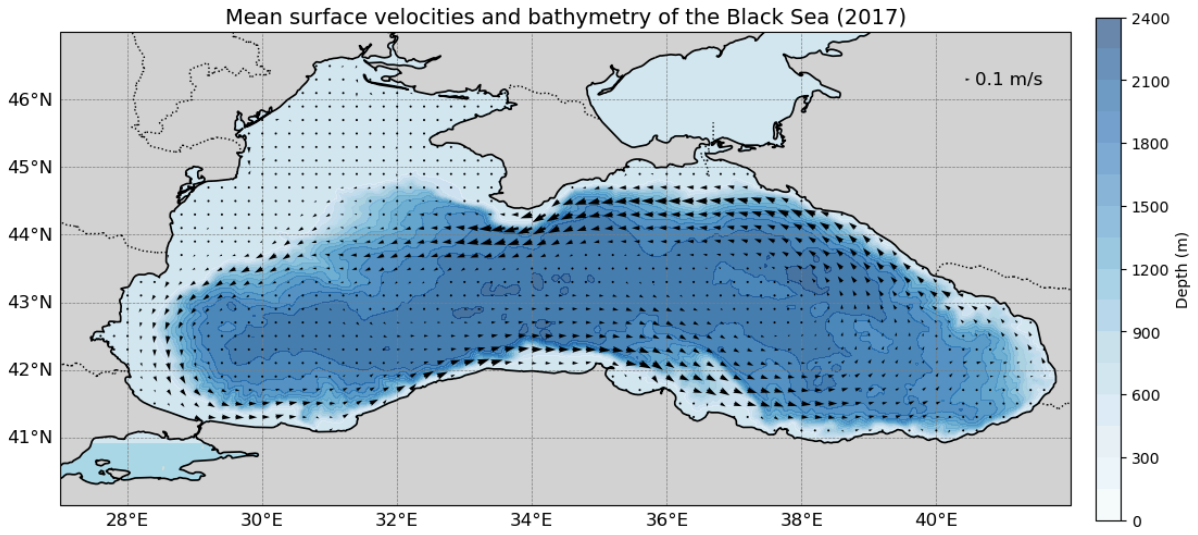

Figure 1 : The Black Sea geography, bottom topography and mean surface currents in 2017 (Data : NEMO).

The Black Sea receives a significant annual inflow of freshwater, estimated at around 300 km³/year, mainly via rivers. This volume represents a significant amount in relation to the total volume of the basin (540,000 km³). These inflows create an imbalance in the Bosphorus Strait, due to its narrow passageway: the "water-loosening" effect of the Bosphorus Strait outgoing water (low in salt) is twice as high as incoming water (higher in salt), which largely explains the Black Sea's characteristic low salinity (Stanev, 2005). The semi enclosed basin also has a negative precipitation-evaporation balance, meaning that there is less fresh water input from rainfall than from evaporation, leading to an increase in salinity. That said, the inflow of water from rivers is still significant enough to maintain the surface salinity of the basin at around 18 PSU. This creates a distinct vertical layering between the surface and the first 100 m and limits the vertical exchanges in the water column. Surface and bottom layer salinities are 18.04 and 35.97 PSU respectively, with salinity entering exclusively through the Bosphorus bottom inflow (Jarosz et al., 2011). Another boundary between the 50-100 m and the deeper waters is the cold intermediate layer, which is created by winter cooling, followed by the spreading of this cold intermediate water mass throughout the Black Sea (Stanev, 2005).

3. *Biodiversity*

The Black Sea's inability to mix vertically makes it the world's largest anoxic - and even euxinic - basin : beyond a depth of 150 m, the water masses contain hydrogen sulphide (Jørgensen et al., 2001 ; Li et al., 2024) and the upper layer is ventilated by air-sea exchange.

Thus, the Black Sea has a thin layer of ~100m oxygen-ventilated water, but the rest of the basin is lacking oxygen (Capet et al., 2016). This anoxic condition combined with a marked stratification in summer make it difficult to develop habitable areas. This complex and isolated environment forces the species living in the basin to adapt in different ways to those of the same species from different populations (Gurielidze et al., 2012).

The majority of phytoplankton in the Black Sea are diatoms (Gurielidze et al., 2012). There are also 171 species of fish, 800 zoobenthic species (molluscs, polychaetes) and a total of 116 species of plankton near the Gregorian coast only (Gurielidze et al., 2012). Bat et al. (2018) used the Red List (IUCN) to count 5 endangered habitats and 1 critically endangered habitat for Black Sea species. In 2017, there were also 7 vulnerable (VU), 2 endangered (EN) and 10 critically endangered (CR) species in this sea, which is already poor in biodiversity (Gurielidze et al., 2012); Bat et al., 2018). It is therefore becoming clear that protecting the waters and, in particular, the territories of the Black Sea, whose waters are becoming increasingly polluted by Marine Litter, is essential.

The Black Sea is becoming increasingly polluted, particularly as a result of tourism, the construction of ever-larger cities along its coasts (BSC, 2007; Aytan et al., 2016; Lechner et al., 2015; Gonzalez-Fernandez et al., 2020), increasingly contaminated waste water, (over-)fishing and the fact that several rivers, passing through several countries, flow into it (Aytan et al., 2020). The threat this thesis is focusing on is the microplastic : where is it accumulating, which processes will affect its distribution and, finally, how will it coincide with the important ecological places in the Black Sea. Indeed, several species ingest microplastic passively, implementing by filtering the water, as in the case of mussels, in which plastic has been found. Due to their availability in various sizes, plastics can be ingested across all trophic levels, from zooplankton to mammals (Aytan et al., 2022; Wright et al., 2013; Şentûrk & Aytan et al, 2024). Plastic pollution represent the large majority of the marine litter found at the sea surface (Suaria et al., 2015; Aytan et al., 2019; Berov & Klayn, 2020), on the beaches (Simeonova et al., 2020; Öztekin et al., 2020) and on the sea floor (Topcu & Öztürk, 2010; Uzer et al., 2020; Kasapoğlu et al., 2020). The dominant part of the isolated plastic particles found in mussels consists of polyethylene (PE) and polyethylene terephthalate (PET), the plastics identified as being the most prevalent in the Black Sea (Ibryamova et al., 2022 ; Pojar et al., 2021; Berov et al., 2020). When microplastic starts to be ingested by plankton, it is transmitted and bioaccumulates in the trophic chain (Toschkova et al., 2024). This is the case, for example, with several species of fish caught in areas of the

southern Black Sea, for which microplastic accounted for the majority (93.2%) of plastic found (Aytan et al., 2022).

Microplastic

1. *Why is it interesting to investigate about microplastic in the Black Sea ?*

The Black Sea, with a high river discharge from several countries into the enclosed basin, provides an exceptional opportunity to study microplastic behavior (D'Hont et al., 2021). Since it is a semi-enclosed basin, particles get trapped in it and make the sea very sensitive to contamination. There is also a high river discharge from several countries, and limited vertical mixing. It receives significant anthropogenic input from riverine and canal discharges originating in heavily industrialized and urbanized regions. These pressures are further amplified by coastal development, intensive fisheries, recreational use, and, in some areas, direct waste dumping. Plastic pollution has emerged as a dominant and persistent form of marine debris in the region, prompting calls for urgent mitigation measures (Aytan et al., 2016; Cincinelli et al., 2021; Goryachkin and Efremova, 2022; Mukhanov et al., 2019).

While the Black Sea's vertical stratification, euxinic deep layers, and limited water exchange influence biogeochemical processes (Capet et al., 2016), studies suggest that microplastic accumulation may not significantly vary across water layers, according to a study in different areas of Denmark, even in the Kattegat/Skagerrak region, which has a strong water stratification as well (Gunaalan et al., 2024). This raises critical questions about the mechanisms such as physical processes like marine currents or biogeochemical processes like plastic degradation, which are governing microplastic transport and distribution. Understanding these dynamics in the Black Sea is essential not only for assessing long-term impacts and identifying key accumulation zones but also for preserving its rich biodiversity and critical habitats, in particular the large northwestern shelf, which have far-reaching implications for conservation.

2. *Definition and generalities*

Since the 1950s, 8.3 billion metric tons of petroleum based plastics have been produced (Geyer et al., 2017 ; Payel et al., 2025). In the last decades, because of its cheap production cost, versatility and ease of processing, the production accelerated. After the pandemic, the policies started to implement way more single-use plastic, which resulted in yearly production of approximately 180 million metric tons of manufactured single used

plastic for a couple of minutes only (Payel et al., 2025 ; Chen et al., 2021 ; Plastic Europe, 2020). In April 2024, the IUCN (International Union for Conservation of Nature) recorded that at least 14 million tons of plastic end up in the ocean every year. Nowadays, the presence of microplastic in the ocean exceeds 51 trillion particles in number, and 3700 (>1 µm in size) particles per m^3 in concentration (Lindeque et al., 2020). While the "Great Pacific Garbage Patch" often symbolizes this issue, the reality is more subtle and alarming—most microplastic particles are invisible to the naked eye, breaking down into fragments small enough to infiltrate marine food webs. These particles pose significant risks to biodiversity, ecosystem health, and human well-being as they accumulate in organisms and ultimately enter our food supply (Sharma et al., 2017 ; Marcharla et al., 2024).

In the marine environment, under the influence of UV radiation, wind, currents or chemical reactions (e.g. oxidative degradation, photodegradation) plastic can break down into small particles. The upper size limits used in research to classify microplastic range from 500 µm to either 1 mm or 5 mm at the upper limit (Desforges et al., 2014; Frias, et al., 2019 ; Thompson et al., 2004). In the ocean, microplastic can float, stay on suspension in the water column or sink, depending on its density. Plastics with a density that exceeds that of seawater (1020 kg/m3), like cellophane and bottles composed of polyethylene terephthalate (1440–1510 kg/m3 and 1380 kg/m3 respectively), sink and accumulate in the sediments (Woodall et al., 2015; Alomar et al., 2017). Polyethylene terephthalate (PET), polypropylene (PP) and polyethylene (PE) are among the most widely used packaging plastics. During their longevity in the environment, these microplastic absorb inorganic and organic pollutants through surface interactions such as dioxins, dichloro diphenyl trichloroethane, polychlorinated biphenyl and so on (Bank & Hansson, 2019; Bradney et al., 2019; Nizzetto et al., 2016). Microplastic has been found everywhere on earth, from the Mariana Trench (Peng et al., 2018) to Mount Everest (Napper et al., 2020) and from zooplankton (Steer et al., 2017) to gigantic baleen whales (Kahane-Rapport et al., 2022).

3. *Degradation mechanism*

In this section, we develop the several types of degradation a plastic that is entering the marine environment will go through. These processes are not considered in the lagrangian simulations of the thesis, since it depends on a lot of parameters that are still very unsure. These simplifications are made in other studies (Castro-Rosero et al., 2023; Miladinova et al., 2020) to focus on the surface transport patterns and to identify one by one the impacts of different processes. However, it is still important to understand the full picture of every

simplification and how in later research, adding degradation processes could improve the accuracy of simulations.

Several processes can alter microplastic that enters the marine environment. Degradation is defined as "*an irreversible process leading to a significant change in the structure of a material, typically characterised by a change of properties (integrity, molecular mass or structure, mechanical strength) and/or fragmentation, affected by environmental conditions*" (Organization for Standardization: Geneva, 2013; Krzan, 2006). Depending on the polymer composition, the plastic will degrade through different biotic or abiotic pathways. The kinetics of its degradation depends on oxygen concentration, water chemistry, temperature, sunlight and degrading microorganisms dynamics (Laycock et al., 2017). Macroplastic degrades first at the polymer surface, a process called "surface erosion", which disintegrates the plastic into smaller pieces – meso-, micro-, nanoplastic and, ultimately, polymer fragments. During the microplastic stage, the surface to volume ratio is higher and, therefore, the degradation process proceeds faster (Gewert et al., 2015). The time scale of these processes is still not well understood and difficult to predict, because of the amount of parameters to test and the difficult conditions to mimic.

Photodegradation is a very common pathway caused by the chromophore defects present in the polymer chain. To be able to absorb light energy, the polymer has to have unsaturated chromophoric groups, but in most cases, additives and impurities such as pigments – which are incorporated in plastic during production – are the main cause of absorption of UVs. Those available spots absorb the UV light (280-420 nm wavelength). It causes the generation of radicals that will degrade in 3 steps called initiation, propagation, and termination (Zhang et al., 2021 ; Payel et al., 2025). During the initiation phase, the C-C or C-H bound breaks due to the UV absorption, forming an alkyl radical R. This alkyl, during the propagation phase, reacts with atmospheric oxygen. The result, ROO, interacts with the polymer chain and will then create hydroperoxide ROO and R. During the termination stage, after the auto-oxidation, the produced radicals can form carbonyl, peroxides and alcohols as an end product (Zhang et al., 2021; Payel et al., 2025). Following photodegradation, the plastic may undergo another degradation process known as thermo-oxidative polymer degradation. The process is similar to photodegradation, but with thermally stable and not light-limited materials (Dimassi et al., 2022). Thermal degradation occurs at elevated temperatures, usually close to the melting point of the specific polymer type (>100 °C) (Booth et al., 2017).

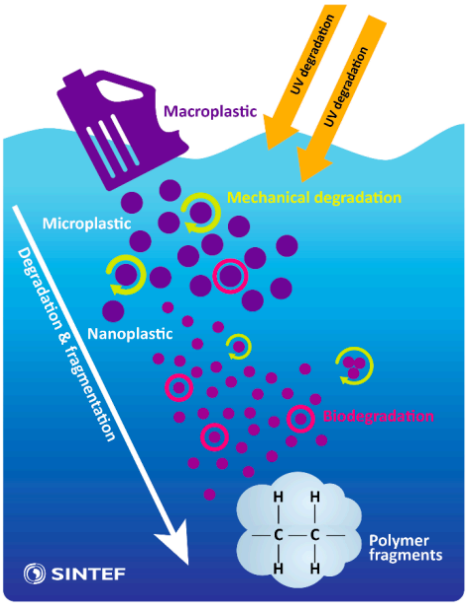

Figure 2 : Overview of the main degradation processes and the fragmentation of plastic items in the marine environment (Booth et al., 2017).

The polymer can also react with water (Annex 1), which causes erosion (surface or bulk). PP and PE are not normally degraded by hydrolysis processes, but PET is. This degradation process splits the polymer chain in two as a result of its reaction with water. If the bonds are stable, the process will be more difficult, whereas if they are labile, the process will go very fast. Hydrolysis decreases with increasing hydrophobicity or molecular weight (Booth et al., 2017; Payel et al., 2025).

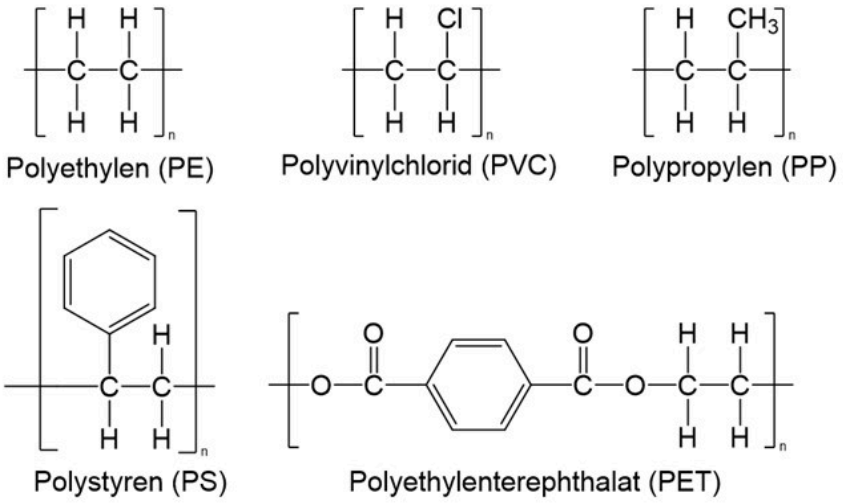

Figure 3 : Overview of the monomer of the 5 most common types of plastic. Binding angles have not been taken into account (Biotech Academy).

Oxidative and hydrolytic degradation processes lead to a reduction in the molecular weight of the polymer chains, which causes the mechanical properties of the material to change and become brittle. Degradation processes that modify polymer structure, molecular weight or polymer chain properties, such as oxidative degradation or hydrolysis, render materials brittle and gradually fragment them. So, if the polymer chain is longer or the intermolecular forces stronger, plastics take longer to erode.

Microplastic are not inert particles; they interact with biological and chemical processes in the ocean. The transport of microplastic can be influenced by biofouling, the colonization of plastic surfaces by microorganisms, algae and organic materials. This phenomenon alters buoyancy and sinking dynamics over time, for example by enhancing aggregation processes (Kowalski et al., 2016 ; Amaral-Zettler et al., 2021). To capture these processes, parameters such as primary production and organic matter flux can be used to model biofouling rates: how much will attach to particles, how its density will change and, thus, how the sinking velocity and its vertical position in the water column will evolve through time (Fischer et al., 2022).

4. *Types of microplastics in the Black Sea*

Marine litter – any persistent manufactured or processed solid material discarded, disposed or abandoned in the marine environment (International Maritime Organization, n.d.; United Nations Environment Programme, n.d.) – can be found under several types of forms, such as metal or, as the main ominous one in the Black Sea, plastic. Jambeck et al. (2015) estimated that up to 1 million tons of mismanaged plastic waste could enter the Black Sea from the surrounding countries (Strokal et al. 2022). As defined and detailed, plastic can undergo different chemical-physical processes in the marine environment and create microplastic. In the Black Sea, the main types of pollutants are from cigarettes, wrappings, plastic bottles, tobacco… (Aytan et al., 2020; Shen et al., 2021; Simeonova et al., 2020). Several studies identified zones in the semi-enclosed basin where plastic could accumulate or stay for a period of time that is difficult to predict : the surface layer, the water column, the sediment and, when it happens, beaches – that is what is called “beaching”. Pojar et al. (2021), studied the plastic concentrations on the Bulgarian and Romanian shelf and estimated that in the surface layer, 1-19 particles/m^3 could be found, with an average of 7 particles/m^3 across the 12 studies. The plastic was collected with a neustonic net of a mesh size of 200 µm.

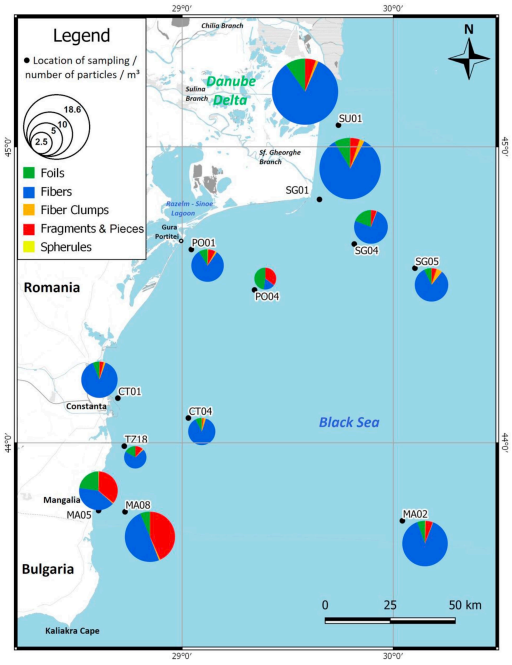

Figure 4 : Map of the study sites in Pojar et al., 2021.

The main polymers present in the water were identified, with polypropylene (PP) and polyethylene (PE) being the predominant types (Pojar et al., 2021; Berov, S., et al., 2020). Due to the high plastic abundance near the mouth of the Danube and the lower concentrations elsewhere along the coast, it is assumed that the Danube is the main source of plastic (Pojar et al., 2021).

5. *Trajectories of the particles*

Once the plastic particles enter the marine environment, their trajectories are impacted by different biophysical forces. It is possible in numerical modelling to simulate those. In this thesis, we consider advection, diffusion, stokes drift, wind forcing and sinking, while paying attention to beaching.

Advection refers to the transport of particles by the bulk movement of ocean currents, effectively carrying them across large distances. Diffusion describes the spreading of particles from regions of higher concentration to regions of lower concentration, driven by random molecular motion or turbulence. While advection is governed by the velocity field of the ocean, diffusion is typically modeled using Fick's Law (Hautala, S., 2020). Following the study by Castro-Rosero et al, 2023, it is considered important, in terms of simulation accuracy, to take into account the impact of waves drift on the transport of microplastic particles. Beyond passive sinking, the model will also consider Stokes' drift, which arises due

to the asymmetry in wave motion, where particles near the surface experience a net forward displacement compared to those at greater depths. This phenomenon could be very significant in the Black Sea, if wind-driven waves enhance horizontal transport and, thus, impact the distribution of floating microplastic.

This transport factor is called Stokes drift – a result of the velocity field generated by the surface gravity waves (Espenes et al., 2024). Advection, diffusion and stokes drift impact the particles at the surface layers and it is common practice to consider them in 2D (Espenes et al., 2024; Onink, V., et al., 2019 ; Delandmeter & van Sebille, 2019).

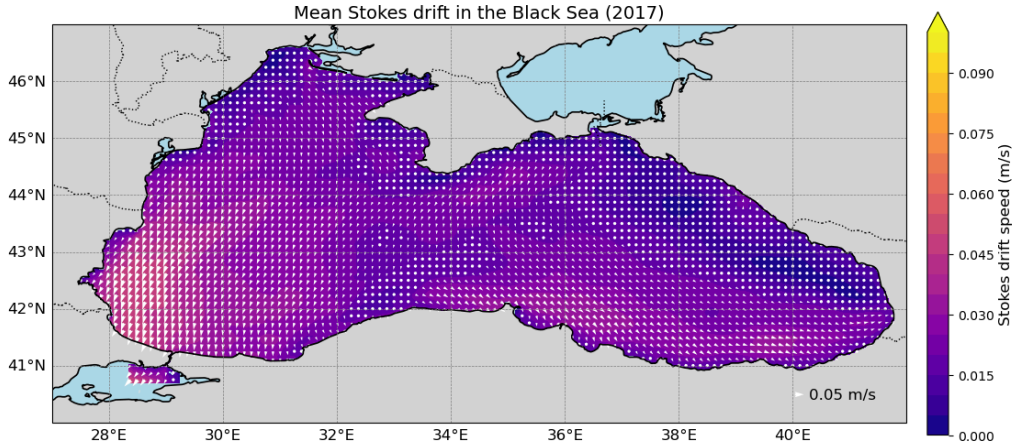

Figure 5 : Mean Stokes Drift velocities at the surface of the Black Sea in 2017 (Data: CMEMS).

Particles in the marine environment can also sink into deeper layers. In the marine environment, biofilms get attached to small particles, such as bacteria, algaes or diatoms and result in a density change, affecting the buoyancy of the particles. In the Black Sea, the highest rates of biofouling were observed during summer and in the middle and deeper layers (Vladimir et al., 2023). However, in this thesis, we only impose a fixed sinking velocity.

Gaps and thesis purpose

Although the transport of microplastic in marine environments has been widely studied using Lagrangian modelling techniques, relatively few studies focus on enclosed seas such as the Black Sea. Only a handful of works (Miladinova, 2020; de Castro-Rosero et al., 2023; Stanev & Ricker, 2019) have investigated with a numerical model the surface transportation of microplastic and accumulation zones in this basin. The three main studies worked solely on physical transportation and demonstrated the importance of adding Stokes Drift to advection and diffusion only. This leaves several knowledge gaps, which needs to be answered methodologically, to be sure of the importance of each process once added. In this

thesis, we will focus on the dynamics of particles in the basin, without considering the fact that they could be fragmented or that they could be degraded. We investigate the impact of adding a sinking velocity to passive particles in the Black Sea. To quantify and analyse our results, we address the following questions :

1. How do vertical transport affect particle dispersion and retention in a semi-enclosed basin with complex bathymetry and deep currents ?
2. To what extent do riverine sources contribute to spatial accumulation patterns, compared to an idealized homogenous input ?
3. Which regions of the Black Sea are most prone to microplastic accumulation, and how does this vary across depth and time ?

This research addresses these current gaps in our understanding of microplastic transport in the Black Sea by simulating particle dispersion using the *Ocean Parcels* Lagrangian framework. By coupling this particle tracking model with outputs from a three-dimensional physical-biogeochemical model (NEMO-BAMBHI), the study investigates key oceanographic processes that influence the movement, accumulation and fate of microplastics.

Materials and methods

This part of the thesis is divided into three sections. First, we describe the tools, followed by the used data and models and, finally, the initial scenarios of plastic particle placement in the Black Sea. We use the data from the NEMO-BAMBHI model with a python package called *Ocean Parcels*. With this library, it is possible to launch simulations with important forces that have an impact on the trajectory of our particles.

Tools

1. Lagrangian simulations and ocean parcels

To be able to follow the trajectory of a particle in a marine environment, we use a lagrangian perspective. It means that instead of choosing one point and seeing what happens through time in that exact position, we are directly following the movement of the particles. It considers the position of a particle (x, y, z) at time t relative to its initial position. This is computed with a simple general equation (1) : We follow the position through time *(x(t))*,

considering the initial position *(x(0))*. We make an integration in time of the velocity field *(v(x(s),s)* to retrieve the final position and, finally, we add an additional behavior *(B(x(s),s))*.

$$x(t) = x(0) + \int_0^t v(x(s), s) + B(x(s), s)\, ds \qquad (1)$$

To be able to follow the particle motion through space and time, we use a package in python called "Ocean Parcels", version 3.1.2. It is an open-source Lagrangian particle tracking tool written in python designed to operate with oceanographic datasets such as current velocities, wind stress, or diffusivity fields, typically derived from Eulerian ocean models (van Sebille, 2019). In our case, we use the NEMO-BAMBHI model (Madec et al., 2017 ; Grégoire et al., 2020). We chose to use Ocean Parcels because it is a widely adopted and well-documented Python framework for Lagrangian ocean modelling. It is also used in many peer-reviewed studies (e.g., Lange & van Sebille, 2017; Delandmeter & van Sebille, 2019; Fischer, 2022) and supports robust numerical schemes like Runge–Kutta 4, offering an increasing user base in the oceanography community.

To start a simulation, we have to load ocean currents and other forcing data like waves and winds. The atmospheric wind data is from ERA 5 (Hersbach et al., 2023) and the wave data is downloaded from the CMEMS data files (Staneva et al., 2022). The simulations are run in Just-In-Time (JIT compilation) mode, since it is faster and easier to use for long simulations with a lot of particles as in our case (Delandmeter, 2019; *Parcels Documentation*).

To run the simulations, you need to have the forcing data, a well-defined *fieldset*, a *particle set* with all the information about the launching and initial data, the *kernels* used – i.e. the physical phenomena imposed on the trajectories – and finally, the order in which the simulation will be run. The position of the particle is updated and registered every 6 h, this is what is called a *timestep* (dt), so that we can follow a precise trajectory over time, without using too much memory and without losing accuracy. We chose a 6-hour timestep following Bouzaiene et al. (2021), who used the same value in the Black Sea and showed that it was sufficient to reproduce key dispersion regimes and match observed drifter data.

One of the core functions of Lagrangian simulation software is to accurately interpolate the gridded velocity fields in both space and time. Since particles move continuously across the domain, while the input data are only defined at discrete grid points and time steps, this interpolation step is essential to compute physically realistic trajectories (Delandmeter & van Sebille, 2019).

In this study, microplastics are considered to be Lagrangian particles and, for modelling purposes, are assumed to be spherical, in contrast to their actual irregular shapes in real conditions. The fact that they behave as idealized virtual tracers is a limitation we accept in this thesis.

When we consider a scenario in 2D, it implies that we do not consider the sinking behavior of particles and their vertical trajectories (Aliani and Molcard, 2003; Zambianchi et al., 2017; Miladinova et al., 2020). They follow the behaviour we impose on them and properties such as shape, density or size are not explicitly imposed. This abstraction allows for a simplified yet useful representation of transport processes at the ocean surface. When we go into 3D and add a uniform sedimentation rate to all the particles, we still do not consider their shape, diameter or density. These parameters are only taken into account when using *kernels* linked to biofouling. In reality, however, microplastic particles do have different shapes, and it is hypothesized in the literature to affect their transport dynamics in the marine environment (Kowalski et al., 2016 ; Amaral-Zettler et al., 2021).

The three main studies conducting Lagrangian simulations in the Black Sea have been limited to two-dimensional computations and without imposed sinking rate, focusing primarily on the influence of Stokes drift. Beyond this, only advection and diffusion processes were incorporated (Stanev & Ricker, 2019; Castro-Rosero et al., 2023; Miladinova et al., 2020).

2. *The different kernels*

In *Ocean Parcels*, a *kernel* is a fragment of code executed at each time step for each particle, modifying its state. It is possible to mathematically add behaviours that we want to impose on our particles and, with it, add accuracy to our simulations with the processes we want to consider. We always considered in which order they should be added in the simulation. In this section, we explain all the *kernels* we added to our simulations and how they are used.

a. Advection

The first *kernel* to be added is advection, defined as the transport of microplastic particles due to the movement of the water itself, rather than to their own diffusive movement. This *kernel* integrates the velocity derived from the output of the NEMO-BAMHBI model. In accordance with *Ocean Parcels* conventions, we defined a *fieldset* using python- dictionaries linking data files (filenames_nemo), variable names

(variables_nemo) and corresponding dimensions (dimensions_nemo). Depth information was extracted to ensure vertical consistency between all fields, particularly for 3D advection and sinking processes.

The evolution of its trajectory is solved numerically by a 4th order Runge-Kutta scheme (2). The position of the particles through time depends on its initial three-dimensional position and the velocity field. At each timestep, this method estimates the particle's future position by evaluating the velocity field at four successive intermediate points within the timestep. These intermediate slopes (k1 to k4) are combined to compute a weighted average velocity that accounts for local curvature in the flow. In practice, *Ocean Parcels* handles this integration internally when the *AdvectionRK4 kernel* is applied, using the velocity components (U, V, W) defined in the *fieldset*. The result is a realistic approximation of particle trajectories under the influence of the NEMO-derived currents.

$$y_{i+1} = y_1 + \frac{1}{6}(k_1 + 2k_2 + 2k_3 + k_4) \qquad (2)$$

where

$k_1 = hf(t_i, x_i)$,

$k_2 = hf(t_i + \frac{h}{2}, x_i + \frac{k_1}{2})$,

$k_3 = hf(t_i + \frac{h}{2}, x_i + \frac{k_2}{2})$,

$k_4 = hf(t_i + h, x_i + k_3)$.

In our simulations, we compare two scenarios, in 2 and 3 spatial dimensions, which involves using two different *kernels*, already incorporated in the parcel library: *AdvectionRK4* and *AdvectionRK4_3D*.

b. Diffusion

To the advection, we add diffusivity processes as a stochastic noise and random displacement of the particles, as in the previous lagrangian simulations in the Black Sea (Stanev & Ricker, 2019; Castro-Rosero et al., 2023; Miladinova et al., 2020). The Fokker-Planck equation, a differential equation, describes the time-evolution of the probability density function (random variable) of the velocity of a particle under the influence of drag forces and random forces (Van Sebille et al., 2018). *Ocean Parcels* uses an Advection-Diffusion *kernel* to compute this behaviour.

$$x(t) = x(t_0) + \int_{t0}^{t} u(x,t)dt + R\sqrt{2Kh\Delta t} \quad (3)$$

where

$x(t)$ is the particle position at time t,

$u(x,t)$ is the local velocity field from NEMO-BAMBHI,

Kh is the horizontal diffusivity coefficient [m²/s],

Δt is the time step,

R is a random vector drawn from a standard normal distribution (mean 0, variance 1) in each direction.

We implemented horizontal diffusion as a constant $Kh = 10\,m^2/s$, as in the simulation of Castro-Rosero et al., 2022. This order of magnitude was estimated based on literature on zonal and meridional absolute dispersion for the Black Sea (Bouzaiene et al., 2021; Ciliberti et al., 2022) and previous sensitivity analysis. We used the *kernel* implemented in the Ocean Parcel library *DiffusionUniformKh*, in which the Kh is assumed to be uniform and the horizontal diffusion is only in 2D. These last two elements limit us spatially. Firstly, we cannot adapt the Kh to local bathymetry or turbulence. Secondly, vertical movements linked to turbulence are not modelled in this case. However, these simplifications are common in lagrangian simulation studies (Stanev & Ricker, 2019; Castro et al., 2023; Miladinova et al., 2020).

c. Stokes Drift

As demonstrated by Castro-Rosero et al. (2023) and Stanev & Ricker (2019), adding the Stokes drift – a result of the velocity field generated by the surface gravity waves (Espenes et al., 2024) – adds accuracy to the simulations. Therefore, we add it to every simulation. The Stokes drift data is from the spectral wave model WAM Cycle 6 (CMEMS), with a resolution of 1/36° x 1/27° and hourly time resolution (Staneva et al., 2022 ; Castro-Rosero et al., 2023). Stokes drift can be added as an additional velocity field.

The net transport induced by surface waves is added here to the advection and diffusion components. Ocean Parcel does not currently include a built-in Stokes Drift *kernel*, so we defined it ourselves using the method described in the Plastic Parcels framework (Delandmeter, 2023). However, the wave model Copernicus WAV only provides surface Stokes velocities (u_s). To include the impact of the waves at depth, we use the proposed model by Breivik et al. (2016), which applies a vertical attenuation function derived from the

linear wave theory. It uses the zonal and meridional Stokes velocity fields (Stokes_U and Stokes_V), as well as the wave peak period (T_p) and local bathymetry. The method uses a Philips wave spectrum to estimate the drift speed at depth. The total velocity of a particle becomes :

$$u\,(x,t) \;=\; u_c(x,t) \;+\; C_s(z) \;*\; u_s(x,t) \qquad (4)$$

where

u_c is the Eulerian current from the ocean model (NEMO),

u_s is the Stokes surface velocity (WAM),

$C_s(z)$ is the depth-dependent attenuation factor, calculated analytically as a function of the wave number (k) and the instantaneous depth of the particle (z) :

$$C_s(z) \;=\; exp(2kz) \qquad (5)$$

with z the instantaneous particle depth (negative downward), and k the wave number computed from the peak wave period *Tp*, using the linear dispersion relation. It is determined numerically, taking into account the decrease in drift with depth. This allows the *kernel* to be used in 2D as well as 3D.

d. Sedimentation

To begin exploring the effects of particle sedimentation, we have extended our simulations to the third dimension by imposing a uniform falling velocity on particles over the entire Black Sea basin. The addition of a constant velocity to an advected particle has been shown to be sufficient to incorporate the effect of gravity to a sinking particle (Nooteboom et al., 2020; Monroy et al., 2017). Numerous studies approached this problem with a similar method, considering particles being transported passively with an added vertical and constant velocity. They suggest that the sinking of particles may be oblique (Siegel and Deuser, 1997; Siegel et al., 2008; Qiu et al., 2014; Roullier et al., 2014; van Sebille et al., 2015). This means that particles should not stay at their initial position at the end of the simulation.

This process is modeled via the *sinking_euler kernel*, which updates particle depth as a function of time. Two velocities were tested in the river inflow scenario: a sinking velocity of 6 m/day, based on the values proposed by de la Fuente et al. (2021) for typical microplastic particles, and a faster velocity of 80 m/day, inspired by the study by Kowalski et al., 2016. Although the latter value is probably unrealistic for the majority of microplastics in the Black

Sea, it enables us to assess the maximum effect that a sedimentation rate could have on their transport. The aim of these tests is to understand the extent to which the vertical component of motion influences particle dispersion and residence time, particularly when combined with advection, diffusion and Stokes drift. This work paves the way for more detailed exploration of processes such as biofouling, which in warm seasons can accentuate sedimentation by increasing the effective density of floating particles.

e. Beaching and added *kernels*

The *fieldset* defines the domain in which our particles are going to run and holds the needed hydrodynamic data to execute particles. In our *fieldset*, we add the current velocities, bathymetry, stokes velocities, diffusion and wind data. The simulations stop running automatically as soon as the particles leave the defined *fieldset*. It is therefore important to add limits and *kernels* to ensure that this does not happen. We use the *kernels CheckSurface, CheckOutOfBounds, CheckThroughBathymetry and DeleteBeachedParticle*. They define the limits at the surface, at the bottom of the Black Sea, and near the coast, where particles will no longer be able to go if there is no current velocity. If they leave the area, they are considered to have *beached*.

Model NEMO-BAMBHI

We use the outputs of the coupled hydrodynamical-biochemical model NEMO4.2-BAMBHI (BiogeochemicAl Model for Hypoxic and Benthic Influenced areas) (Madec, G., et al., 2017 ; Grégoire, M. et al., 2020), delivered as a reanalysis product by Copernicus Marine Service (CMEMS) Black Sea Marine Forecasting Center (Grégoire et al., 2025). NEMO (Nucleus for European Modeling of the Ocean) is a three dimensional ocean circulation model that solves the primitive equations of fluid dynamics forced by thermodynamic boundary conditions (Madec et al., 2017). The horizontal components of the current (u and v) are solved from the equations of motion (Madec, et al., 2008). This work is based on the circulation resulting from the NEMO v4.2 model, with a spatial resolution of 1/36° x 1/27° and a daily time resolution (Lange & van Sebille, 2017; Nooteboom et al., 2020). The model is run at a horizontal resolution of 2.5km with 59 vertical levels (Chevalier et al., 2025).

Simulation scenarios

In this section, we define the several scenarios we used to write down our simulations. All our simulation runs for the year 2017 for us to be able to compare our results to the previous studies (Miladinova, 2020; Stanev et al., 2019 & 2022; Castro-Rosero et al., 2023) and to use the plastic data provided for that year (Strokal et al., 2022). Moreover, the system reaches equilibrium within a year of simulation, as the accumulation patterns stabilize and are noticeable after 3 months and the spatial distribution does not significantly evolve when the model is run for a longer period (Miladinova et al., 2020). Thus, running the simulation over a one-year period ensures that the principal physical processes of the Black Sea can complete their characteristic cycles, especially the annual cycle of surface currents and gyres (~1 year), and the renewal processes of intermediate and deep waters (several months to a year) (Stanev, 2005).

We define two types of experiments with the aim to assess the contribution of a sinking velocity and to analyze the different accumulation patterns and their connection with the period and position of the release sites (Castro-Rosero et al., 2023).

1. *Homogeneous distribution*

A first scenario investigated in this thesis is a homogeneous distribution in the semi-enclosed basin. With this first simulation, we can determine the existence of accumulation patterns resulting from surface currents, the seasonal variations and identify the areas with the greatest concentration. Two distinct simulation types were conducted in this scenario, one incorporating an imposed sinking rate of 80 meters per day (3D), the other excluding it (2D). In both simulations, the beaching module is activated, and Stokes Drift is incorporated with Advection and Diffusion. The details of those *kernels* are defined in the second section of Material and Methods, “The different kernels”. We can then compare the impact of adding a dimension and a sinking velocity to a 2D-scenario.

As in the studies of Miladinova (2020), Stanev et al. (2022, 2019) and Castro-Rosero et al. (2023), a hundred particles are released monthly in the year of 2017 and, in our case, they are launched every 15 km (Figure 6). 24,540 particles are released before the end of the year in total. Since this is a conceptual test and that it has been done in literature in the Black Sea, we consider this amount appropriate.

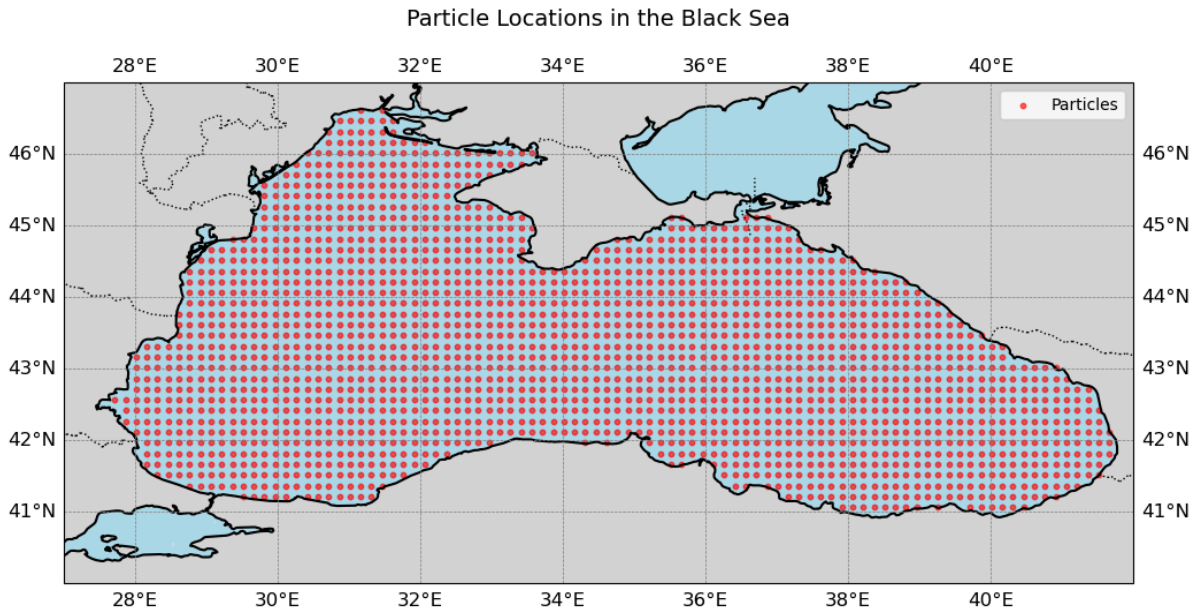

Figure 6 : Initial plastic particle locations for the simulation in the Black Sea homogeneous scenarios (every 15 km).

2. *Rivers mouths as a starting point*

The second scenario aims to be more realistic and considers the main sources of microplastic in the semi-enclosed basin, the rivers. In order to provide the most realistic estimate possible of each river's contribution, we focus on those with the greatest run-off. Castro-Rosero et al. in 2023 describe in their paper how they computed the amount of particles ending up in the basin depending on the river inflow data from the Global Run-off Data Center (GRDC). In order to be able to compare our results with previous research, and to ensure that we are starting from a good base for simulation with the sinking rate, we use the same monthly microplastic inputs at the mouths of the selected rivers: Dnieper-Bug (DB), Dniester (DN), Danube (DA), Sakarya (S), Kizilirmak (K), Yesilirmak (Y), Çoruh (C), Rioni (R), and Don-Kuban (DK) (Figure 9). After a year, 13,901 particles are launched in the simulation (Figure 7).

In this scenario, as described in the “Tools – The different kernels” section, we will compare two different sinking velocities – 6 m/day and 80 m/day. This experience aims to highlight the different behaviour depending on the impact of gravity or other processes that could make a plastic particle sink. It should also show if it is relevant to compute more precisely those processes, or if a fixed velocity is enough to point out the regions in which plastic particles will accumulate.

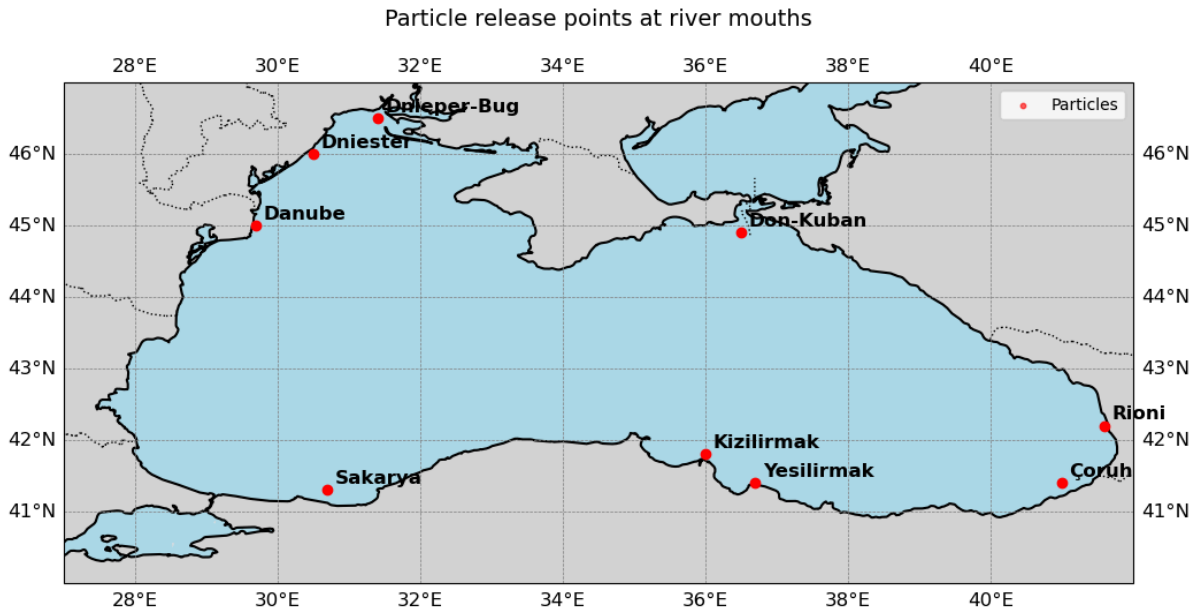

Figure 7 : Initial plastic particle locations at the river mouth for the simulation in the Black Sea riverine inputs scenarios (Based on Castro-Rosero et al., 2023)

Plastic data

Microplastic exports from rivers to the Black Sea were estimated using values from Strokal et al. (2022), which provide annual loads in kilotonnes (kt/year) for the year 2010. Following the methodology of Castro-Rosero et al. (2023), these annual fluxes were converted into a monthly number of released particles, proportionally to the river discharge seasonality derived from the Global Runoff Data Center (GRDC). The idea is to reflect the natural variability in plastic input throughout the year.

Stroke et al., 2022 **Model (kt/year)**		**Rivers selected**	**Annual discharge (GRDC) [m3/s]**	**Quantity exported by rivers [kt/year]**	**Latitude (°N)**	**Longitude (°E)**	**Simulation assumption quantity [kt/year]**
Danube River	0.71	Danube	6468.4	0.71	45.0	29.7	0.71
Dnieper River	0.33	Dnieper	1351.7	0.33	46.5	31.4	0.40
The Don River	0.23	Don	788.5	0.23	44.9	36.5	0.4
Southern rivers	0.84	Sakarya	185.6	0.13	41.1	30.7	0.13
		Kizilirmak	200.9	0.14	41.7	36.0	0.14
		Yesilirmak	185.4	0.13	41.4	36.7	0.13

		Çoruh	197.7	0.14	41.6	41.6	0.14
		Rioni	408.5	0.29	42.2	41.6	0.29
Other rivers	0.49	Bug	110.32	0.07	-	-	-
		Kuban	369.32	0.23	-	-	-
		Dniester	324.32	0.20	46.0	30.6	0.20
All rivers	2.6	-	-	-	-	-	-

Table 1: Amount of plastics exported by the main Black Sea rivers (kt/year) according to Strokal et al., 2022, annual discharge data (m^3/s) according to Global Runoff Data Center (GRDC) data, location of selected discharge points (longitude in °E and latitude in °N) and amount of plastic exported by each point assumed for the simulation (kt/year). Table from Castro-Rosero et al., 2023.

To perform this conversion, we assume, like Castro-Rosero et al. (2023) that one modelled particle represents 200 kg of marine litter. The total number of particles to be released in a year is calculated by dividing the annual load (in kg) by this unit mass. This annual total is then redistributed monthly, using normalized monthly discharge fractions specific to each river. Our values are almost the exact same one as in the previous cited article. Particle injection occurs at the first valid velocity point in the NEMO simulation domain, starting from January 1st, 2017, which is the first available timestamp in our forcing dataset. This results in a variable number of particles released each month, depending on the seasonality of river discharge and the magnitude of plastic exports (Table 1; Figure 8).

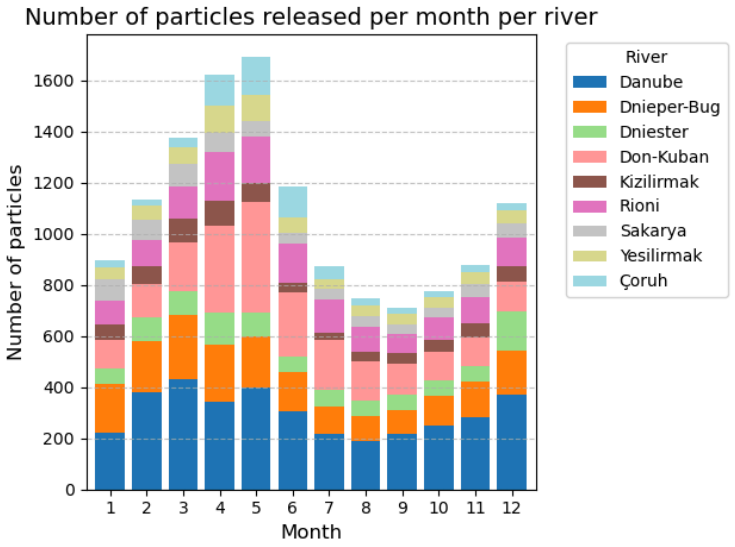

Figure 8 : Number of virtual particles released per month per river, computed with the river flow and based on the article from Castro-Rosero, et al., 2023.

Results

This master thesis investigates the trajectories of particles in the Black Sea to understand the behaviour of microplastic on a large temporal scale – one year– in 2017 in a large but known marine environment – The Black Sea.

This section presents the outcomes of Lagrangian simulations evaluating microplastic transport in the Black Sea. Two main scenarios are compared: one with particles constrained to surface transport (2D), and another including a constant sinking velocity (3D). By analyzing spatial patterns, vertical profiles and beaching behavior, we assess how sedimentation alters dispersion and accumulation zones. We consider that the accumulation zones are areas where particles will run aground or create high density at sea.

Homogeneous release scenarios

The homogeneous monthly release scenario intends to observe the dispersion of particles as if they were already in the sea. This allows us to visualize trends over the year in particle behavior due to the effects of advection, diffusion and stokes drift. Comparing this result with the same scenario, where a sedimentation velocity is added (80m/day), enables us to quantify the effect of this velocity on the distance traveled, the quantity of particles stranded, and their residence time in the sea.

1. *Spatial distribution of particles in 2D and 3D*

Following the approach of Castro-Rosero et al. (2023) and Stanev & Ricker (2019), we compute the particle density as the number of particles per square kilometer to evaluate the accumulation at various locations (Figure 9 A,B). For each month, all recorded particle positions are used. The Black Sea is divided into a regular grid of 100 x 100 bins between 27-42°E and 40-47°N. The actual surface area of each cell is calculated using geodesic methods (WGS84 ellipsoid), resulting in cell sizes of approximately 96 +- 3km² (ranging from 90 to 101 km²). The number of particles in each cell is then normalized by its area to obtain a density in particles/km². It is important to note that the absolute values of particle density depend directly on the chosen grid cell size, which is not standardized across studies. Therefore, our comparisons focus more on relative spatial patterns than on absolute magnitude.

Note that each particle contributes equally to the density calculation, regardless of its release date. As a result, particles released late in the year (e.g. in December) have had less

time to travel or *beach*, but are still considered in the final spatial distribution. This choice may lead to an underrepresentation of their actual dispersal potential.

In the 2D simulation (Figure 9A), the highest particles densities were recorded in October in the southwestern basin, near the Turkish coast (between 40°–42°N), with 3.8 particles/km², and in December in the northeastern areas (off the Russian shelf) with 3.62 particles/km². In contrast, the mean density in this scenario is 0.074 particles/km² over the year, and the median value is 0.033 particles/km². This implies that local maxima are roughly 50 to 100 times higher than the basin-wide average, highlighting strong spatial heterogeneity and suggesting that certain regions act as accumulation hotspots rather than reflecting a uniform distribution of particles.

Over the course of the year, particles gradually disperse throughout the basin, largely following the main currents of the Black Sea. In June, accumulation begins to appear along the Turkish coast in the southwest, while other particles appear to be following the Rim current, a cyclonic (counter-clockwise) and basin-wide current in the Black Sea. In July and August, small zones of accumulation form close to the coast in the southern Black Sea and in the northwestern sector, near the Bulgarian and Georgian coasts. At the end of the year, the area with the highest densities is in the northeastern region of the basin, near the Azov Sea (Figure 9A).

Conversely, the northwestern shelf, along the Romanian and Ukrainian coastlines, shows low particle densities, despite being a region with low current velocities. This may indicate a more efficient offshore export in this region, or early beaching not captured at the surface.

In contrast, the 3D simulation (Figure 9B), which includes a sinking rate of 80 m/day, displays a more homogeneous spatial distribution of particles. The particle densities are computed as for the 2D scenario. Note that these density maps are computed by projecting all particle positions onto the horizontal plane, regardless of their depth. The results represent column-integrated particle densities rather than purely surface concentrations. These maps allow us to identify temporal and spatial hotspots of surface plastic concentration throughout the year.

Higher accumulation is observed along the western coast, from Bulgaria down to Turkey, as well as along the Georgian shelf. Accumulation near the center of the basin also increases, suggesting reduced lateral transport once particles begin to sink.

The largest peaks occurred in November at 43.641(lat)-29.5(lon), and this high density peak also occurred in October with 6.07 particles/km² and December with 6.6 particles/km² at the same location. The other largest peak occurred in July near the Turkish coast with a value of 7.11 particles/km². These density peaks are nearly twice as high as the maxima recorded in the purely 2D experiment (~ 3.8 particles/km²), but still within the same order of magnitude. This suggests that allowing particles to sink reduces immediate coastal beaching, leaving more particles available to accumulate offshore, which may explain the higher localized concentrations observed.

While the 2D trajectories showed particles following the Rim current's cyclonic circulation, the 3D scenario shows shorter and more clustered particle paths, especially in the southwestern and southeastern regions, due to rapid sinking (Figure 12B). Interestingly, the Turkish shelf exhibits higher densities at the end of the year in the 3D simulation, which were less visible in 2D. Similarly, the northwestern part of the basin, initially sparse in the surface-only case, shows greater particle presence in 3D, possibly due to slower offshore advection at depth.

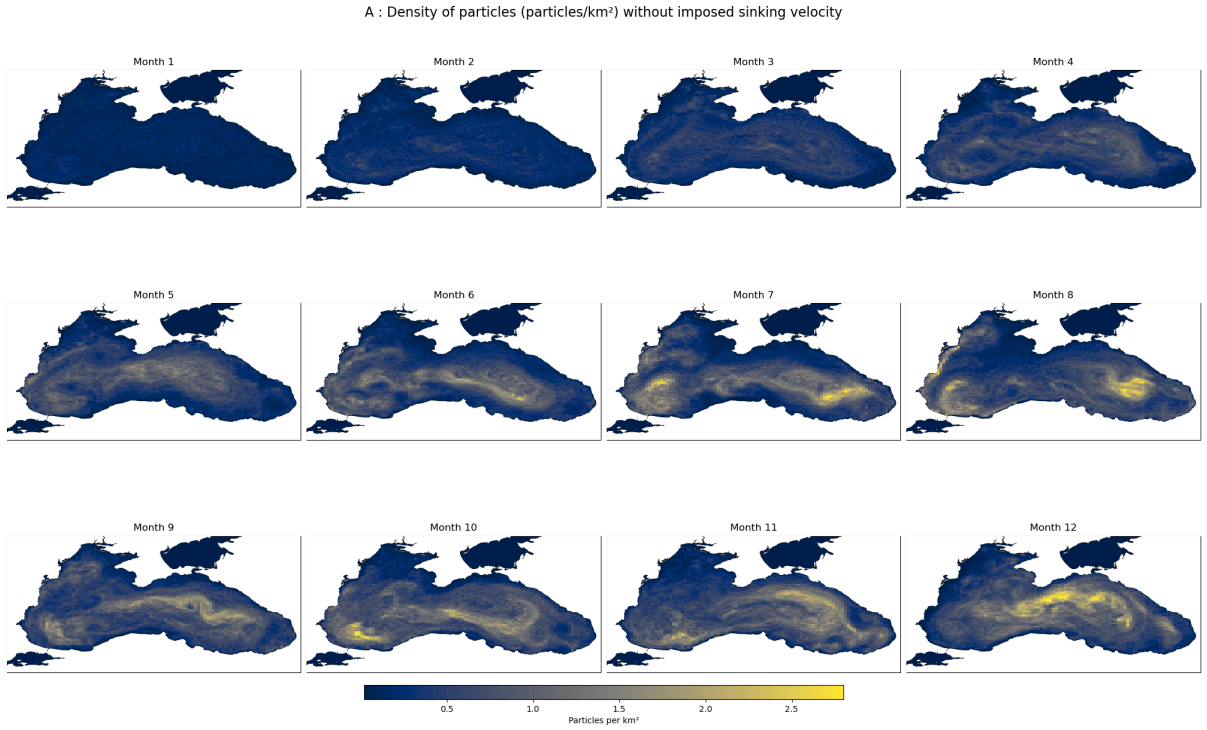

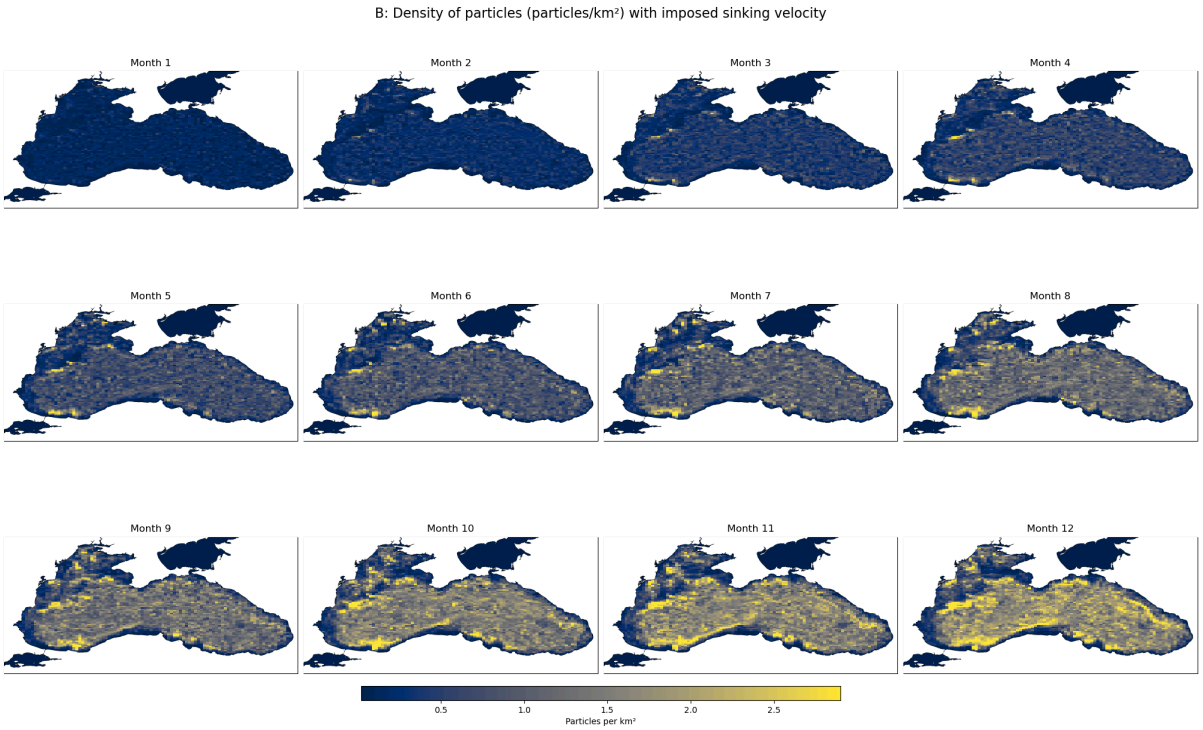

Figure 9 : Comparison of particle density peaks with and without w_sinking (as in the figure from Castro-Rosero et al., 2023). Particles are added every month at every defined spot in the methodology. (A) Distribution of the particle density (particle/km²) at the end of every month without an imposed sinking rate. (B) Distribution of the particle density (particle/km²) at the end of every month with an imposed sinking rate of 80 m/day. The calculation involves integrating over depth to obtain a concentration per unit area.

To better visualize particle trajectories, we randomly selected 20 particles released during the homogeneous simulation and tracked their movement throughout the year. The plastic particles were color-coded according to their quadrants of origin: southwest (SW), northwest (NW), southeast (SE), and northeast (NE) (Figure 10A,B).

In the 2D simulation, the trajectories closely follow the cyclonic Rim Current, with particles circulating counter-clockwise along the basin's periphery. There are also areas where particles follow small eddy trajectories in the Black Sea gyre zones, notably in the eastern gyre.

In the 3D simulation, its structure and intensity are noticeably weaker than in the 2D scenario. Instead of broad horizontal displacement, particles tend to follow short, clustered, and vertically constrained paths. Small "knot-like" trajectories can be seen here, showing the impact of a rapid sedimentation rate on particles (Figure 10B).

A : Trajectories of 20 particles in 2017 without an imposed sinking rate

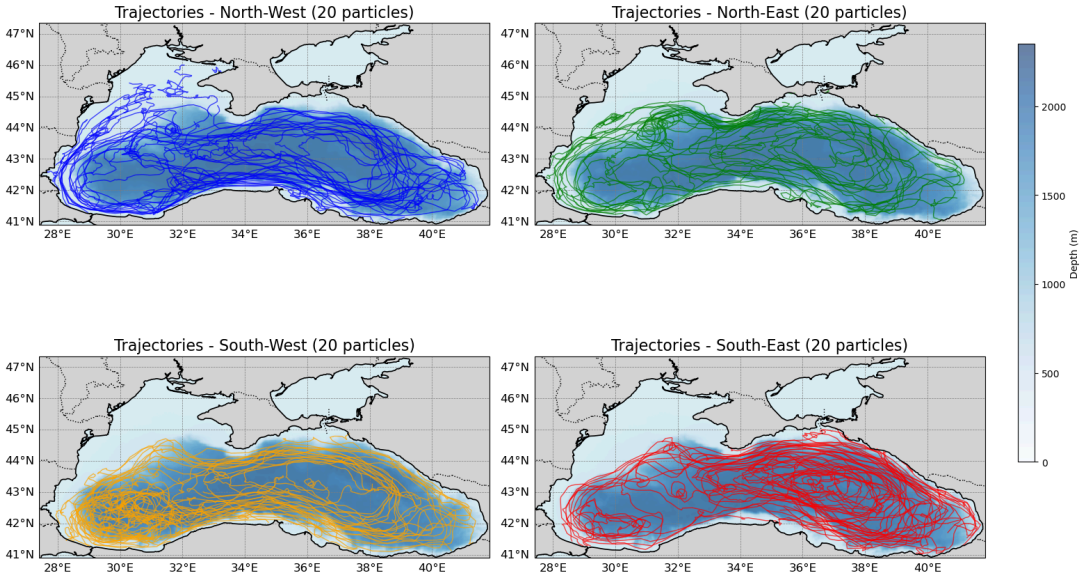

B : Trajectories of 20 particles in 2017 with an imposed sinking rate

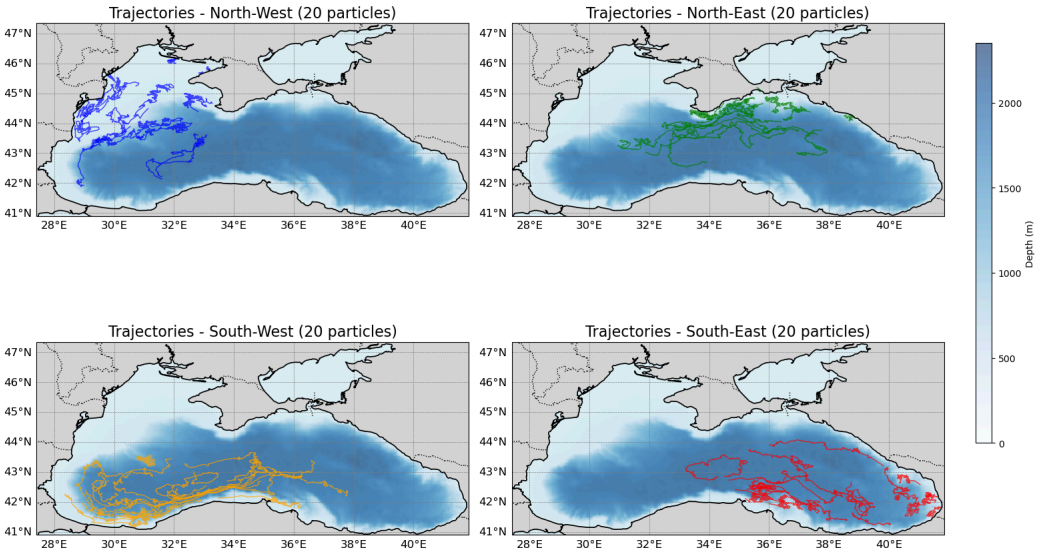

Figure 10 : Trajectories of 20 random particles (fine line) to see how they move (A) Without an imposed sinking rate. (B) With an imposed sinking rate of 80 m/day.

To further quantify the influence of sinking, we analyzed the final position of particles in December relative to their release quadrant (Figure 11). Particles released later in the year (e.g. November) are also considered in the computation.

A clear tendency for particles to remain within their original quadrants is observed in the 2D scenario, with 56.4%, 33.3%, and 48.5% of particles from the NW, SW and SE quadrants respectively staying within and being the predominant amount of particles in their own region. This pattern does not hold for the NE quadrant, where only 25.4% of particles remained in their original area, while 50.2% were originally from the SE quadrant. Similarly, in the 3D scenario, the majority of particles stayed within their starting quadrant: 89.0% in the NW, 73.0% in the SW, 82.2% in the SE, and 65.6% in the NE. We can see that when the sedimentation rate is added, more particles tend to stay in their quadrants. This trend is particularly marked in the SW quadrant, where the proportion of particles originating from the same quadrant increases significantly between experiments — from 33.3% in the 2D release scenario to 73.0% in the 3D release scenario — suggesting that a majority of particles remain within their origin region in the south of the Black Sea, on the Turkish and Bulgarian coasts.

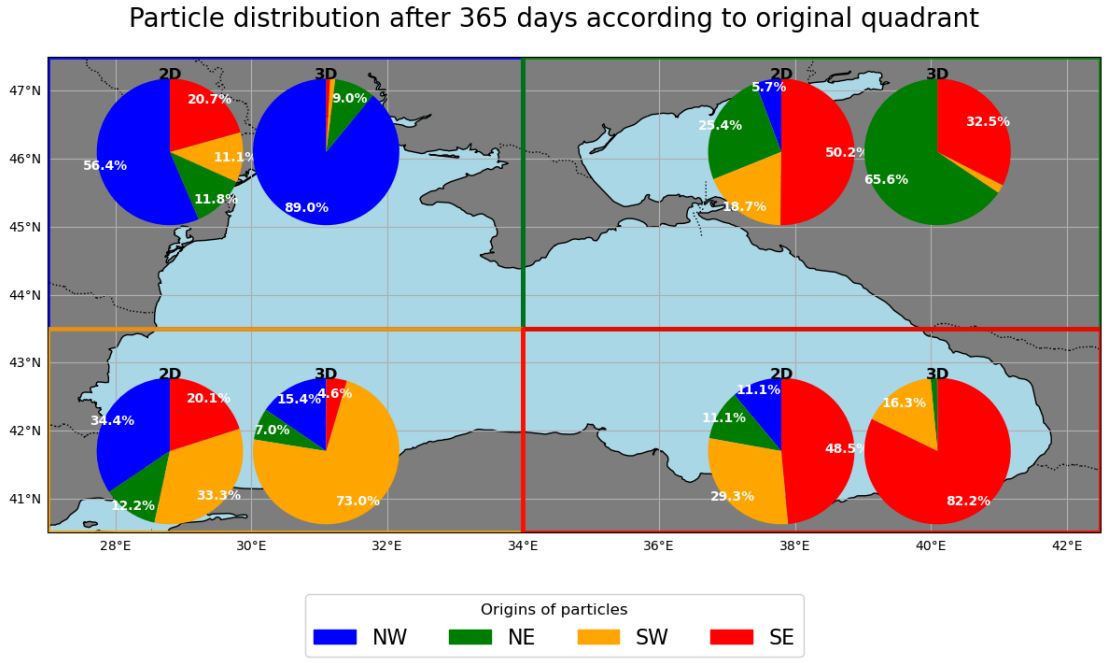

Figure 11 : Distribution of accumulated particles by quadrant according to origin, for the homogeneous 2017 simulation with and without sinking velocity (2D and 3D). Pie charts are placed in the corresponding grounding quadrant. The colors indicate the quadrant of origin of the particles: Southwest (SW) in orange, Northwest (NW) in blue, Southeast (SE) in red, and Northeast (NE) in magenta. Percentages represent the relative proportion of origins in each grounding quadrant and are not written when below 2%.

This pattern suggests that vertical sinking substantially limits horizontal dispersion, increasing the likelihood that particles remain near their source region. As particles sink, they

leave the faster surface currents and enter slower subsurface layers, which strongly reduces horizontal transport and promotes local retention. In both scenarios, particles from the northwestern quadrant, off Romania and Ukraine, rarely reach the eastern basin, while those originating in the northeast show widespread dispersal in the 2D case but more localized patterns in 3D. This emphasizes the role of subsurface current weakness in restricting particle movement across the basin once sedimentation begins.

2. *Depth range with imposed sinking rate*

We trace the vertical trajectory of particles with a sinking rate of 80 m/day (Annex 2). It is important to note that the time axis in the depth evolution plots refers to the number of days since each particle was released, not a fixed simulation calendar. Therefore, all particles begin at day 0, even if they were released in different months of the year (Figure 12, Annex 2).

Particles from each quadrant follow distinct sinking trajectories. In the simulation, once the particles exit the defined hydrodynamic *fieldset*, they are registered as *beached*. At this point, they are removed from the simulation and are not re-injected into the water column (Methodology – Tools). It typically takes 25-30 days for particles to reach the bottom in the deeper parts of the basin. However, some particles do not exceed 200 m depth during the first 90 days (e.g., Northwestern quadrant, Annex 3). This apparent stagnation is linked to the shallow bathymetry of the shelf and limited offshore transport in this zone (Figure 1). In such cases, particles can ground at relatively shallow depths. As long as horizontal currents are higher than 0.0 m/s, particles will still be transported, otherwise they will be deleted (considered *beached*).

Even though the sinking speed is prescribed, the vertical trajectories often display oscillatory patterns (Figure 14). Basin-wide mean vertical velocities indicate that, between 0 and 2000 m depth, vertical velocities can reach up to 0.28 m/day (Figure 13). Such values could be significant compared to the imposed sinking rate, and can account for the observed oscillations in the water column. However, the vertical velocities are difficult to validate in oceanographic models and the explanation between these oscillations in the water column should be investigated.

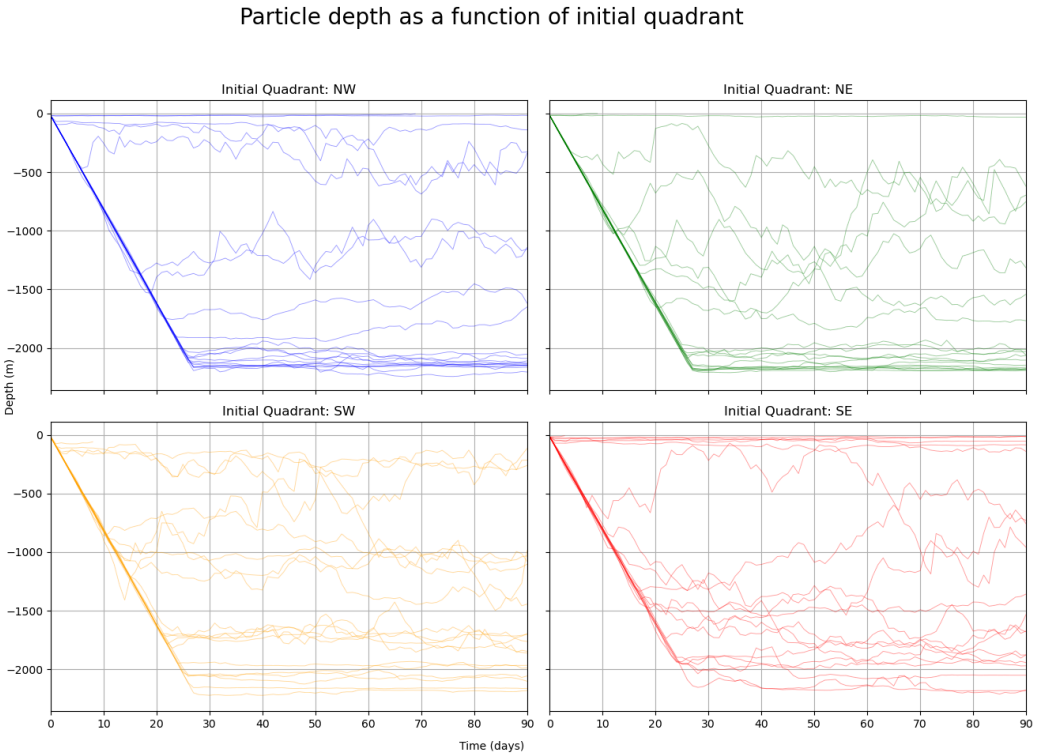

Figure 12 : Depth range reached by 20 particles in the homogeneous scenario with an imposed sinking rate of 80m/day. The colors indicate the quadrant of origin of the particles: Southwest (SW) in green, Northwest (NW) in purple, Southeast (SE) in light blue, and Northeast (NE) in magenta. The day 0 is when the particles are added.

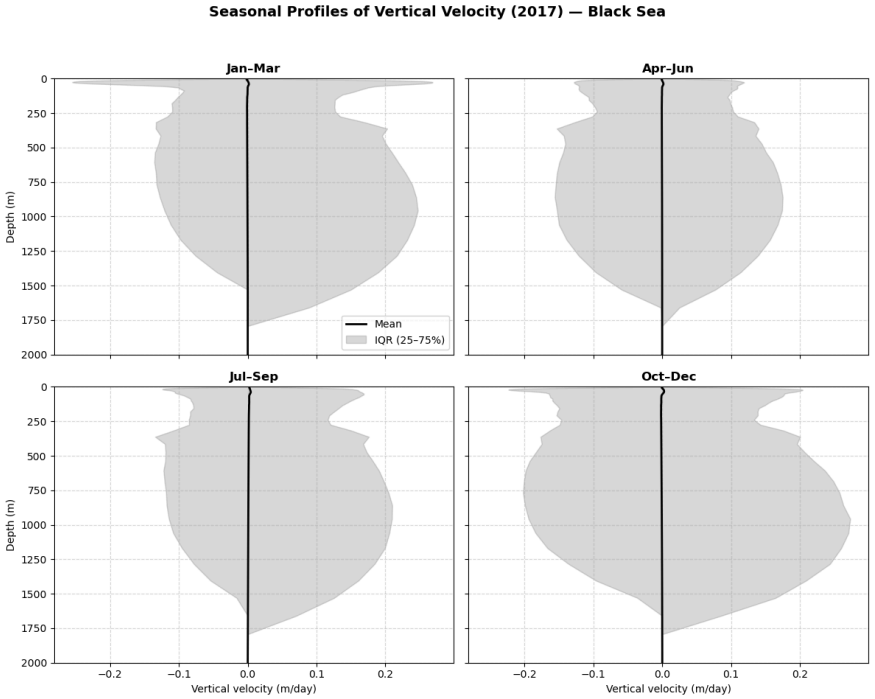

Figure 13 : Vertical velocities (m/s) in the Black Sea in 2017 in winter (January-March), spring (April-June), summer (July-September) and autumn (October-December). Data from the NEMO-BAMBHI model.

Despite these short-term oscillatory movements, particles tend to cross the 500 m depth threshold and remain below it (Annex 4). This is reflected in the monthly distribution of particle depth, which shows that the majority of particles consistently reside below 500 m, except for the northwestern quadrant where the bathymetry is shallower. This vertical pattern reflects the interplay between local bathymetry, vertical turbulent mixing, and the circulation of the upper water column.

3. *The lifetime of particles : travelled distance and beaching*

We consider a particle to be *beached* when it leaves the domain of the defined *fieldset*, as defined earlier in this thesis. When this occurs, *Ocean Parcels* records its last valid position, and the particle is removed from further advection. For this analysis, we use the quadrants boundaries to describe the spatial distribution of particles. The quadrants are delimited with the same boundaries as those in Figure 11.

By analyzing where and when particles beach, we can identify areas with higher retention potential and better understand transport limitations across the basin. In both scenarios, at the end of the year, more than 90% eventually beached during the 12 month simulation (Table 2).

In the 2D scenario, the beaching distribution by quadrant is: 24.32 % of particles from the NW, 13.66 % from the NE, 33.53 % from the SE, and 26.07 % from the SW quadrants. In the 3D simulation, in every quadrant, those numbers decrease : 23.59 % in the NW, 13.04% in the NE, 24.65 % in the SW, and 32.08% in the SE. This decrease underlines the role of vertical sinking in reducing lateral dispersal and enhancing proximity to coastal regions, particularly along the steep eastern margins of the basin. This is marked by the drop from 97.58% to 93.35% of total beached particles (Table 2) : adding sinking velocity reduced the proportion of beaching.

We also calculated the average distance (km) and time (days) before beaching, based on the full simulation period. However, these values must be interpreted with caution. The averages include particles released as early as January 1st and as late as December 1st. Therefore, some particles may have had only 30 days of trajectory before the simulation ended and are counted as “alive”. Others may have not yet stranded but are effectively stopped by the simulation’s time limit. This methodological choice is justified by prior studies, which suggest that a one-year simulation captures most of the relevant basin-scale dynamics (Stanev & Ricker, 2019; Castro-Rosero et al., 2023).

In the homogeneous release without an imposed sinking rate, particles travel large distances. The distance covered is calculated by summing all the short distances recorded over time. Positions are recorded and updated every 6 hours. Particles from the eastern side of the basin travel the most, with an average distance of 1542.61 km and 1525.83 km in the 2D scenario. They also take the longest average time before being considered stranded : 116.28 and 115.07 days. These results align with the dominant Rim Current which efficiently transport surface particles along the cyclonic path around the basin, which we could observe on their trajectories (Figure 10).

In contrast, the 3D scenario produces shorter horizontal transport distances for all quadrants, ranging from 335.92 km (NE) to 359.36 km (SW). Particles on the western side of the basin travel the greatest distance. On average, particles take between 150 and 170 days to run aground, which is slightly longer than in the scenario with no imposed sedimentation rate. This longer residence time may reflect the fact that once particles sink, they experience weaker horizontal currents and take longer to reach coastal boundaries. In both scenarios, the maximal time before beaching was 364 days, no matter the initial quadrant, corresponding to the end of the simulation period.

The bathymetry strongly modulates this dynamic. In the southeastern Black Sea, the steep continental slope allows particles to sink rapidly in deeper layers. As a result, in the 3D scenario, they descend in layers where the horizontal currents are weaker, thus travel shorter distances and beach more locally. In contrast, in the southwestern quadrant (along the Bulgarian and western Turkish coasts), the bathymetry is shallower, and surface current velocities are stronger.

Quadrants	**Average distance travelled (km)**	**Number of beached particles (out of 24,540)**	**Min. time before beaching (hours)**	**Average time before beaching (days)**
2D				
North-West (NW)	1161.17	5,969	0.16	91.35
North-East (NE)	1525.83	3,351	0.083	115.07
South-West (SW)	1362.61	6,397	0.04	101.43
South-East (SE)	1542.61	8,228	0.04	116.28
Total (beached)		23,945 97.58 %		

3D				
North-West (NW)	388.96	5,788	0.41	146.91
North-East (NE)	335.92	3,199	0.04	158.13
South-West (SW)	385.37	6,050	0.04	160.62
South-East (SE)	359.36	7,872	0.04	163.04
Total (beached)		22,909 93.35 %		

Table 2 : Results of the analysis of the average distance traveled of particles [km], number and percentage of particles beached (%), minimum and average [days] beaching time for each type of simulation (with and without an imposed sinking rate, respectively 2D and 3D) according to their source quadrant (Inspired by Castro-Rosero et al., 2023).

In summary, the interplay between sinking rate, bathymetry and current structure explains the observed contrast between east and west. In deep eastern regions, particles sink deeper and travel less. In shallower western regions with strong surface currents, particles are retained in shallower water with horizontal currents and therefore travel greater distances. This is especially the case in the 2D scenario, where particles can only be horizontally advected, and where particles from the NE and SE travel the highest distances.

Riverine input scenario

The scenario with the addition of rivers now allows us to visualise the dynamics of particles from more realistic sources. Here, we analyse the same elements as before: densities, times and distances travelled, and we also compare the impact of two different sedimentation speeds imposed. This allows us to assess their combined influence on particle dispersion, accumulation zones and dynamics. It also provides insight into the role of land-based inputs in shaping the basin-wide pollution patterns.

1. Spatial distribution of particles with different sinking rates

We visualize particle trajectories from river sources in both sinking scenarios : one with an imposed sinking velocity of 6 m/day, and another with 80 m/day (Figure 14 A,B). Overall, particles released from river mouths tend to remain closer to their source than in the homogeneous scenario, and the Rim Current structure is not clearly observed in either case. This reflects both the limited initial distribution area and the rapid sinking, which reduce the exposure time to large-scale horizontal currents.

At a low sinking rate (6 m/day) (Figure 14A), particles sink at a smaller rate and stay longer in the waters with higher horizontal currents. As a result, they exhibit longer trajectories, with recognizable patterns in regional gyres. In the southern basin (41.7°-31°), near the Sakarya River (Turkey), particles follow a vortex-like loop consistent with the Sakarya gyre. The same is true of the Sevastopol gyre, where particles follow trajectories similar to those of the surface circulation. Particles from the northwestern region follow the stronger currents, which transports them towards the southern part of the basin.

In contrast, under the higher sinking rate of 80 m/day (Figure 14B), the trajectories are shorter and more localized: only a few of the Sakarya and Don-Kuban rivers reach the center of the basin and turn slightly into what is starting to look like a gyre. This confirms that higher sedimentation rates limit lateral dispersion, reinforcing localized retention close to river mouth.

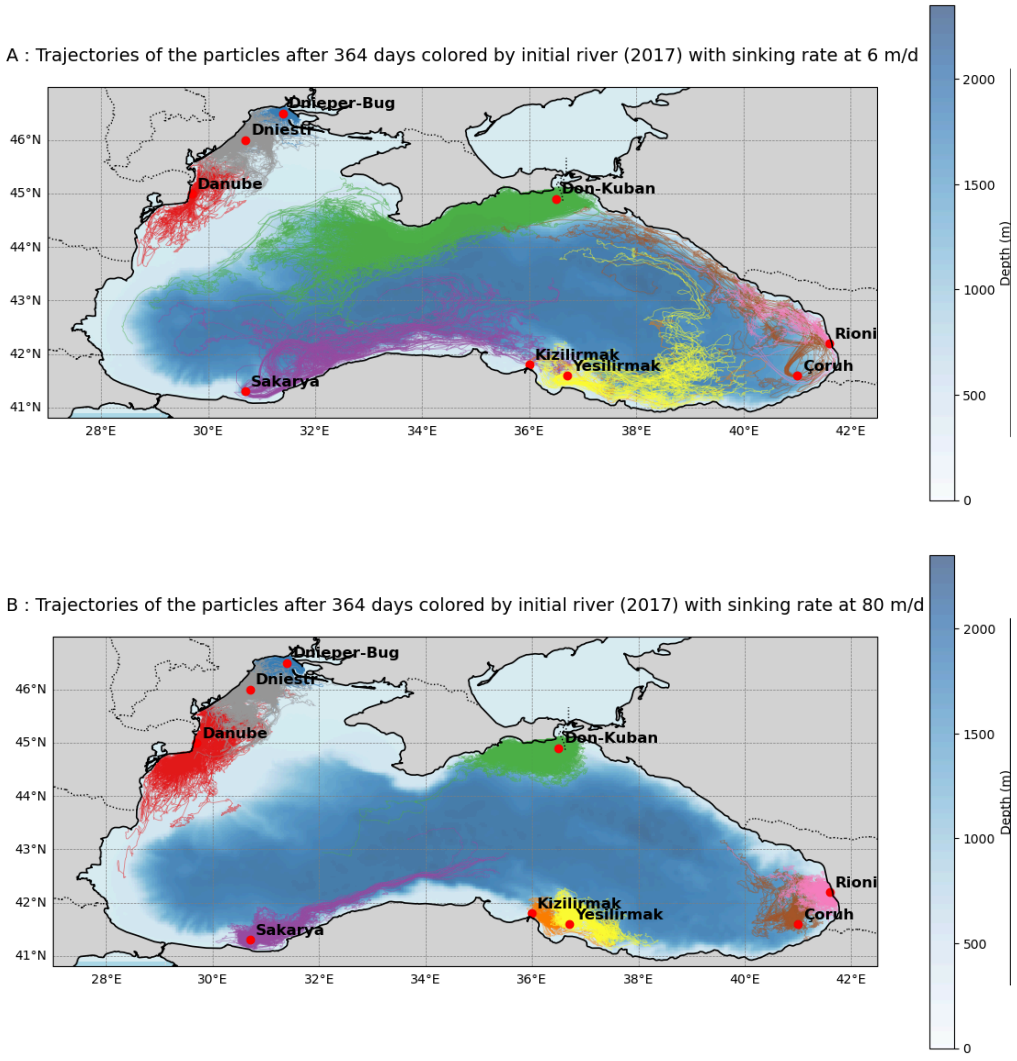

Figure 14 : Trajectories of the particles at the surface starting from the main rivers.

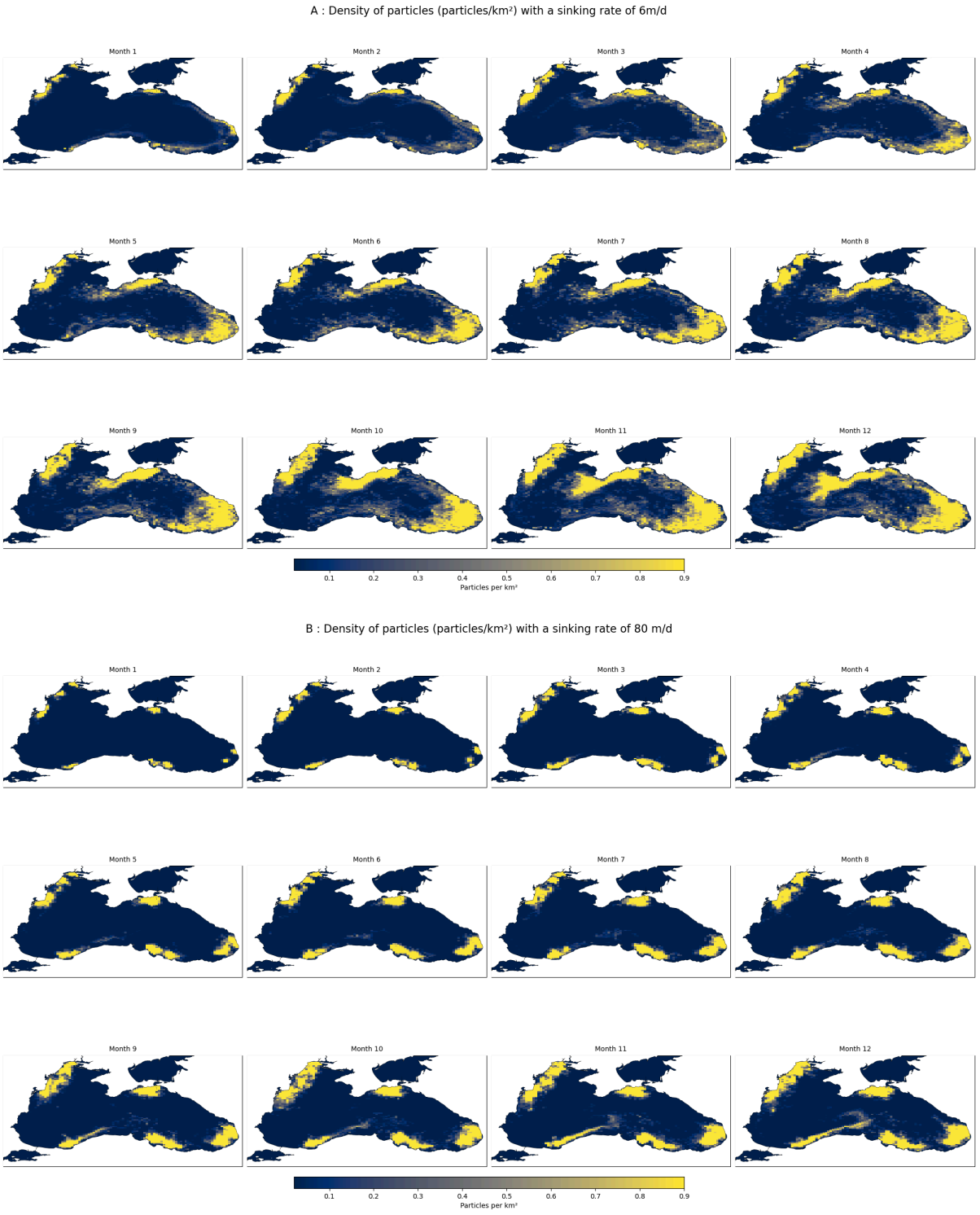

Figure 15 : Particle density [particles/km²] resulting at the end of each month of 2017 with the simulation made with particle release from the 9 chosen rivers. The calculation involves integrating over depth to obtain a concentration per unit area. The Masmara Sea and the Azov Sea are taken into consideration. (A) With a sinking rate of 6m/day. (B) With a sinking rate of 80m/day.

To quantify accumulation, we computed monthly particle densities (particles/km²) for both sinking scenarios (Figure 15). It is computed the same way as for Figure 9 : the Black

Sea is divided into a regular latitude-longitude grid (99 x 99 cells). The actual surface area of each cell was calculated with a geodesic projection. For every month, all particle positions were counted in each grid cell and then normalized by the cell area. Note that these density maps are computed by projecting all particle positions onto the horizontal plane, regardless of their depth, exactly as for the homogeneous (3D) scenario.

As expected, the abundance of particles is significantly higher at the surface when the sinking velocity is low (6 m/day). The slower descent allows particles to remain longer in the surface layer, where they can be advected and accumulate in convergence zones. The plots show a progressive darkening over time, indicating increasing accumulation in specific areas –especially around river mouths and gyre structures.

Compared to the homogeneous release scenario, riverine inputs lead to much higher local density peaks. At 6 m/day, maximum densities reach 45.8 particles/km² in June near 44.9°N, 36.6°E (off Crimea, close to Sevastopol), with other peaks observed around 46.5°N, 31.5°E (northwestern Black Sea, near the Danube delta, Romania/Ukraine) during winter and spring. At 80 m/day, maxima are stronger and more persistent, exceeding 65 particles/km² between May and July near the Crimean coast, and remaining above 40 particles/km² until the end of the year.

2. *Depth range with imposed sinking rate*

We traced the vertical profile of released particles from each river mouth to analyze how the imposed sinking rate interacts with circulation and bathymetry (Annex 5). As for the homogeneous scenario (Figure 12), the time axis starts at t = 0 day for each particle upon release, meaning that particles released in December have less time to descend than those from January.

In both simulations, particles tend to sink rapidly in deeper waters with the bathymetry. However, differences in their depth trajectories are observed depending on their river of origin, even though all particles are subjected to the same imposed sinking rate. This suggests that local hydrodynamic conditions, such as surface advection and vertical velocity, play a significant role in modulating their position.

In the simulation with a sinking rate of 6 m/day, particles remain longer in the upper water layers. For example, particles from the Danube sink gradually and only reach depths below approximately 120m after 60-80 days. In contrast, in the second scenario with a sinking rate of 80 m/day, particles sink faster and reach deeper layers earlier, where horizontal transport is limited due to slower subsurface currents. As a result, particles can

only begin to sink significantly once they are advected offshore, into regions where the seafloor lies deeper.

In the simulation with a sinking rate of 80 m/day, the descent is much faster: particles from rivers in the southwestern region (Kizilirmak, Yesilirmak, Çoruh) reach depths of 1000-1500 m within just 20 days. Notably, Sakarya particles descend all the way to the seabed (~2000 m) in about 60 days, making them the only ones to reach the bottom in this scenario. In contrast, particles released from the Rioni, Sakarya, and Don-Kuban rivers tend to stabilize at shallower depths.

Furthermore, although the imposed sinking rate dominates vertical displacement, small-scale vertical velocities and eddy motions could lead to vertical oscillations. These oscillations may explain why some particles temporarily stabilize at certain depths or display non-linear descent patterns. However, the typical vertical velocities in the model are an order of magnitude lower than the imposed 80 m/day (Figure 13), which could explain why this scenario shows more predictable and rapid vertical penetration, relatively independent of the river's origin. Vertical velocities reach up to 0.2 m/day in some areas of the basin in some areas of the basin (Figure 13). Although this is small compared to the imposed sinking speed of 6 m/day or 80 m/day, it may still influence particle trajectories locally, particularly through oscillatory movements. An investigation to compare the oscillations more precisely in the two scenarios would help to confirm the importance of vertical velocities in the basin and their impact on particle trajectories as a function of the imposed velocities.

In summary, the difference observed between rivers in terms of depth reached are not caused by variations in the sinking rate itself, but by a combination of bathymetric constraints, horizontal advection, and local vertical dynamics, which delay or accelerate the descent depending on the hydrographic context.

3. *The lifetime of particles : travelled distance and beaching*

Although overlapping trajectories sometimes make it difficult to visually assess particle movement, the particles travel substantial distances before beaching. In the scenario with an imposed sinking rate of 6 m/d, the longest average travel distances were observed for particles released from the Sakarya river (746.70 km), followed closely by those of the Çoruh river (727.03 km), and the Kizilirmak and Yesilirmak (approximately 680 km).

In the simulation with the imposed sinking rate of 80 m/day, particles travelled shorter distances overall. The longest average distances were covered by particles from Yesilirmak, Çoruh and Kizilirmak, with average distances of 436.83 km, 424.59 km and 398.13 km

respectively (Table 3). The values obtained from distance travelled calculations are consistent with the results obtained, described and shown in Figures 16 and 17.

By the end of the simulation year, 13,901 particles had been released from the river mouths. In both simulations, the percentage of stranded particles per river ranged from 4.9% to 27.5% in the 6 m/day case, and from 4.6% to 27.3% in the 80 m/day case. These values indicate that, despite the difference in sinking rate, the overall beaching rates remain quite similar across scenarios (Table 3).

At the end of the year, as in the scenario with a homogeneous distribution of plastic in the Black Sea, more than 90% of the particles are stranded. Mean times to particle stranding also remain similar in both scenarios, with the exception of the Rioni River, where the mean time to beaching drops from 113 days to 68 days between the two simulations.

Rivers	**Average distance travelled (km)**	**Amount of beached particles**	**Min. time before beaching (days)**	**Average time before beaching (days)**
Sinking velocity = 6 m/day				
Danube	315.67	3,829	0.04	76.16
Dnieper-Bug	102.13	2,129	0.83	48.70
Dniestr	276.76	1,054	3.29	88.84
Kizilirmak	683.04	775	0.08	169.16
Çoruh	727.03	688	6.41	208.96
Rioni	426.27	1,540	1.04	112.99
Sakarya	746.70	775	1.67	171.97
Yesilirmak	675.75	750	1.79	179.96
Don-Kuban	594.63	2,360	6.79	176.42
Sinking velocity = 80 m/day				
Danube	203.46	3,790	0.04	61.46
Dnieper-Bug	106.87	2,128	1.95	53.81
Dniester	254.74	1,034	5.42	90.11
Kizilirmak	398.13	693	0.16	178.68
Çoruh	424.59	639	30.0	208.97
Rioni	121.10	1,495	0.29	68.25

Sakarya	385.21	718	6.0	155.95
Yesilirmak	436.83	680	7.16	186.49
Don-Kuban	352.12	2,218	14.29	174.45

Table 3 : Results of the analysis of the average distance traveled of particles [km], number of beached particles, minimum and average [days] beaching time for each type of simulation (with an imposed sinking rate, respectively 6m/day and 80 m/day) according to their river of origin (Inspired by Castro-Rosero et al., 2023).

Discussion

In this section, the results of the Lagrangian simulations are interpreted in light of previous research on the Black Sea. To investigate the relative importance of vertical transport and riverine inputs, we added sinking velocities to our scenarios (Table 4). It is important to remember that particles are considered by the simulation as passive tracers, passively transported by the circulation fields, meaning they do not have a dynamic reaction to their environment.

We compare our results to literature and then explore how different sinking velocities influence accumulation patterns, beaching, and the spatial distribution of plastic particles in the Black Sea. With our results, it is possible to estimate important ecological zones to protect from this growing threat and open new discussions about how to perfect the 3D simulations in the Black Sea.

Dimensions / Name	**Sinking velocity**	**Number of particles**	**Physical processes considered**	**Duration**
Scenario 1 : Homogeneous				
2D / 1-2D	No sinking velocity	24,540	Advection, Diffusion, Stokes Drift, Beaching	1 yr
3D / 1-3D	80 m/day		Advection, Diffusion, Stokes Drift, Imposed Sinking, Beaching	
Scenario 2 : Riverine input				
3D / 2-6SV	6 m/day	13,901	Advection, Diffusion, Stokes Drift, Imposed Sinking	1 yr
3D / 2-80SV	80 m/day			

Lagrangian Simulations in the Black Sea in Literature				
Study	**Scenario**	**Nbr. of particles**	**Physical processes considered**	**Duration**
Zlateva et al., 2024	Bulgarian coast and riverine input ; 2D	5000	Advection, Diffusion, Stokes Drift	1 yr
Castro-Rosero et al., 2023	Homogeneous & Riverine Input ; (2D)	11,004 Monthly flow (Strokal et al., 2022)	Advection, Diffusion, with and without Stokes Drift	1 yr
Stanev & Ricker, 2019	Homogeneous & Riverine Input ; 2D	45,000 Same for all rivers, monthly flow	Advection, Diffusion, Stokes Drift	1 yr
Miladinova et al., 2019	Homogeneous, Danube, Istanbul ; 2D	12,000 /yr	Advection, Diffusion	1 yr

Table 4 : Summary of our experiments and literature experiments.

Accumulation patterns and comparison with literature

As a result of our Lagrangian simulations, in which we dropped particles monthly over a homogeneous distribution or at the river mouths, we produced maps identifying accumulation zones based on particle density (particles/km²). These zones reflect where particles tend to converge and eventually beach. Our results align with other studies in the Black Sea (Table 4), while also revealing subtle spatial variations.

2D scenario

The 2D scenario is the most comparable to previous studies, since it is the one without sinking velocities. In this scenario, particles are distributed predominantly according to the general circulation of the Black Sea, with maximum concentrations located mainly in the southwestern (SW) and northeastern (NE) zones of the sea. These accumulations correspond to the accumulation zones described by Stanev & Ricker (2019), who also observed a significant concentration point in the area near the Bosphorus to the west and on the Russian coast to the east. In particular, the formation of an accumulation zone in the southwest, corresponding to the cyclonic dynamics that govern surface circulation (Figures 9, 10), is a point of convergence confirmed by several studies (Zlateva et al., 2024; Castro-Rosero et al., 2023). The simulations of Zlateva et al. (2024) for 2021 estimated surface retention densities of up to 55 items/km² per grid cell per day in the southwestern Black Sea. This metric represents an accumulation rate of floating macrolitter and is linked to the persistence of

particles in coastal waters. Such high retention values are likely explained by specific recirculation patterns in the western gyre of the Black Sea, reinforced by the semi-permanent Rim Current and the local eddies of the Bosphorus and Sakarya. Such circulation features have been shown to favour particle retention and localized convergence zones (Stanev and Ricker, 2019; Zlateva et al., 2024).

Our simulation also indicates that a substantial proportion of particles remain within their initial release quadrants, particularly in the northwestern (NW, 56.4 %) and southeastern (SE, 48.5 %) areas. This persistence can be attributed to the weak cross-gyre transport, consistent with the mesoscale eddy structures and boundary currents described in earlier work. Since more than 90% of particles beached in the homogeneous scenario, it is also possible that the proportion staying within the initial quadrant is that they beached there.

3D scenario

The introduction of a sedimentation rate modifies this spatial distribution: particles show a more marked tendency to remain in their quadrant of origin, with proportions reaching 89.0 % in the northwestern quadrant, 65.6% in the north-east, 73.0 % in the south-west and 82.2 % in the south-east. This strong retention suggests that vertical sinking substantially limits horizontal dispersion by moving particles into deeper layers where horizontal current velocities are generally weaker. Although advection continues at depth (Figure 16) –the reduction in current strength limits cross-basin transport, leading to enhanced accumulation near the coasts, particularly along the western margin. An investigation could show if this is possibly due to stronger trapping by coastal currents as suggested by some studies (Nooteboom et al, 2020; Jalón-Rojas et al., 2019; Monroy, et al., 2017; de la Fuente et al., 2021).

In the homogeneous release scenario, particles generally follow trajectories shaped by the Rim Current, with cyclonic loops and gyre-like patterns emerging at various times of the year. This confirms, in line with previous studies, that advection is the primary driver of microplastic transport in the Black Sea. When a sedimentation rate is imposed, particles initially sink below the surface and are advected by the weaker currents (Figure 16). Many retain a trajectory aligned with the large-scale basin circulation. This demonstrates the persistent influence of the Rim Current structure, even at 100 m depth, where horizontal currents can reach 0.2 m/s (Figure 16) whereas vertical velocities can at best reach 0.00003 m/s (Figure 13).

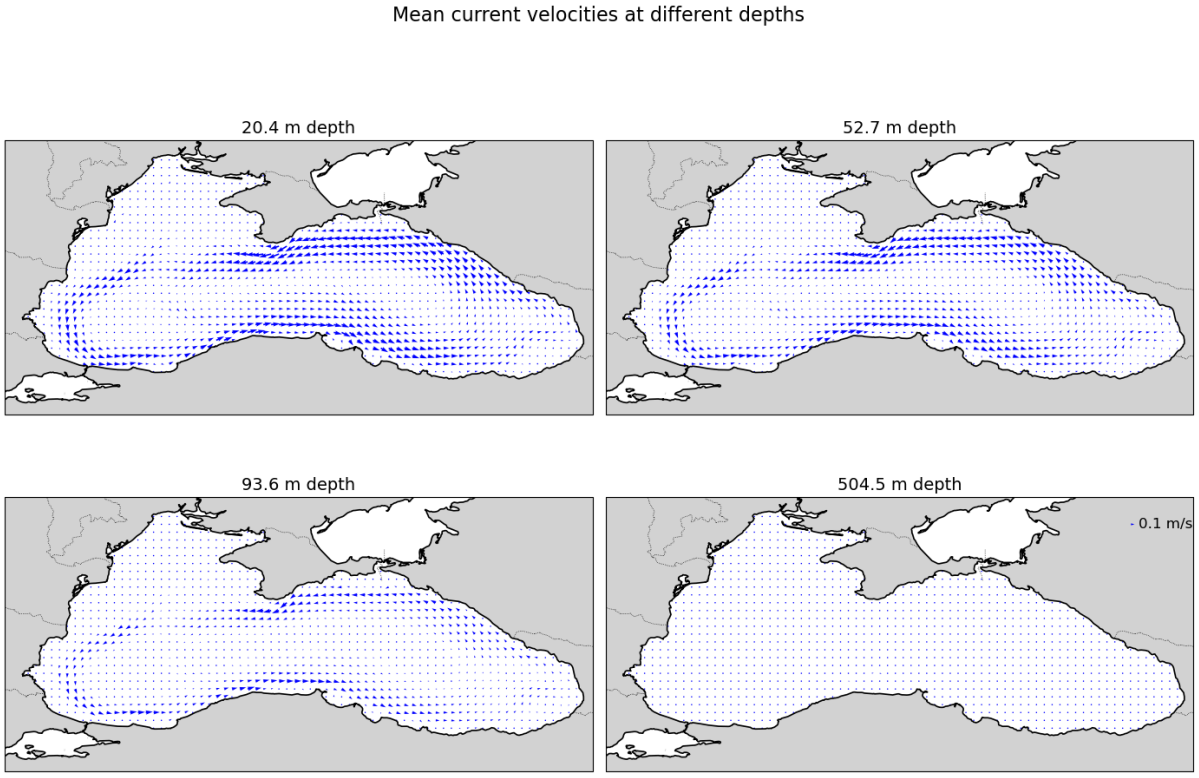

Figure 16 : Mean current velocities at different depths in the Black Sea (20.4 m, 52.7 m, 93.6 m and 504.5 m). Data from the NEMO-BAMBHI model.

In comparison, the release scenario from the nine main rivers shows highly localized accumulation zones around the river mouths, particularly near the Danube, where particle density is the highest. This observation is in line with the results of Castro-Rosero et al. (2023), Stanev and Ricker (2019) and Miladinova et al. (2020), who emphasize the importance of river inputs in the local concentration of floating waste. In the scenario with an imposed velocity of 80 m/day, the majority of particles do not follow major currents such as the Rim current at the surface, and remain essentially close to their source of origin. This confirms limited dispersion and low interaction between zones. However, few particles go towards the center and follow the deep water circulation, ending in zones with weak horizontal currents (Figure 16).

In summary, our results indicate that accumulation dynamics are highly dependent on the release mode, since the homogeneous scenario favors wide dispersion with accumulation zones linked to general circulation, while the river scenario shows strong localization around river sources with little lateral dispersion, reinforcing the importance of integrating specific river inputs into models to better understand and manage critical microplastic accumulation

zones in the Black Sea. That said, we can see that lateral displacements are strongly impacted by the addition of sedimentation velocity.

Vertical transport : Depth range with imposed sinking velocities

As the particles sink, they can always be transported horizontally, a lateral transport that is not negligible in the case of low sedimentation speeds (Nooteboom et al, 2020; Jalón-Rojas et al., 2019; Monroy, P., et al., 2017; de la Fuente et al., 2021). These studies show that microplastic can sink and accumulate in the deeper layers into the water column. In our two experiments, with the homogeneous distribution scenario and both river scenarios, we observed that our particles, even if they sink, continue to move laterally. Nooteboom et al., (2020) demonstrate the importance of mesoscale phenomena on the transport of Lagrangian particles. Their results show that the presence of gyres in currents, which are large-scale phenomena, has a significant impact on the lateral transport of particles flowing in the water column. They tested two sedimentation speeds on Lagrangian particles, estimating the sinking velocity of marine snow and diatoms at 25 m/day and 6m/day, respectively. The average distances travelled ranged from a hundred kilometres to almost 600 km horizontally on average. As expected, a faster sedimentation rate led to a more limited horizontal dispersion range, since particles are advected by slower currents in the deeper layers. However, when turbulent diffusion was included—mimicking the effect of subgrid-scale eddies— the horizontal spread of the particle distribution increased slightly, in agreement with previous findings (Nooteboom et al., 2020).

In our case, this is also observed: in all 3D scenarios, regardless of the sinking velocity, particles in the northwestern quadrant– where the mouth of the Danube, Dniester and Dnieper are located– travel longer distances. This is because their descent is constrained by the local bathymetry: in shallow shelf areas, particles can only sink until they reach the seabed, after which they will remain subject to horizontal transport or beach. While suspended in the upper layers (0-200 m depth; Figure 16), they are still exposed to energetic currents, including the Rim Current, which induces lateral advection and would explain why particles from the northwestern quadrant cover longer distances. In some cases, particles are laterally advected away from the shelf into deeper parts of the basin, where the seabed lies deeper. There, the descent time is considerably longer, and particles continue to be transported horizontally before eventually reaching the bottom. This mechanism is especially

pronounced in the southwestern sector, where upper-layers currents are stronger than in the northwest (Table 2; Figure 16)

Interestingly, although the sedimentation rate was imposed as constant, we observed vertical oscillations in many particle trajectories, with some particles sinking and then temporarily rising. As particles are advected laterally while sinking, they cross regions of upward and downward velocities (Figure 13), which can temporarily displace them vertically. A related phenomenon has been described by Monroy et al. (2017), who showed that even when particles experience a steady sinking speed and the velocity field is incompressible ($\nabla \cdot u = 0$), vertical and horizontal clustering can emerge due to the fine-scale structure of oceanic flows—such as mesoscale eddies and filaments (Monroy et al. 2017). These structures can orient particles along complex three-dimensional trajectories, inducing zones of divergence and convergence that lead to local accumulation or dispersion. The interaction between vertical sinking and lateral advection means that particles move through layers of different velocities, potentially being dragged upwards or trapped in rotating vortices that induce oscillatory movements (Monroy et al. 2017). In our case, however, the oscillations simply reflect the imprint of the resolved circulation field on otherwise passively sinking particles. Further investigation to understand the dynamics and cause of the oscillatory movements is needed.

De la Fuente et al. (2021) studied the dynamics of rigid particles suspended in the water column, considering sedimentation velocities from 6.20 m/day to 68.21 m/day. In their model, particles sink without moving significantly away from their point of origin, which can be explained by the absence of biological interactions or fragmentation, factors not taken into account in their simulation, and also absent from our own simulation. Their results show that sedimentation speed has a strong influence on the time it takes for particles to reach the bottom of the Mediterranean Sea. For example, for a sinking velocity of 68.21 m/day, particles take around 21.8 days to reach the seabed. By contrast, when the velocity drops to 6.20 m/day, the sedimentation time increases considerably, reaching almost 247 days. These results are comparable to our own, in which plastic particles sink in 20 days in the deep waters of the Black Sea at an imposed speed of 80 m/day. At lower imposed velocities, sinking is substantially prolonged, and lateral advection becomes an important control on their distribution.

The work of Kaandorp et al. (2020) models the fate of floating plastic in the Mediterranean over a decade (2006-2016) and shows that around 45% of plastics end up sinking in the water column, while 54% run aground on the coast. In their study, sinking is

parametrized as a probabilistic process linked to biofouling, whereby initially buoyant particles progressively acquire a higher likelihood of sinking. This approach leads to high estimated sedimentation fluxes near the coast, with values in excess of 1 kg/km²/day, reflecting a rapid loss of buoyancy immediately after emission. In the open sea, fluxes are lower, but still significant, with values between 0.1 and 1 g/km²/day, particularly in areas influenced by gyres or strong current structures. These fluxes are expressed in terms of mass, whereas our results are expressed in number of particles per unit area. A direct comparison is therefore not possible without assumptions about particle size and density. Nevertheless, our simulations show a similar dynamic: particles from rivers in the southwestern Black Sea (Kizilirmak, Yesilirmak, Çoruh) reach the bottom of the basin in around twenty days. While this metric is not a mass flux, it points to sedimentation timescales of the same order as those inferred by Kaandorp et al. (2020). This concordance reinforces the idea that the vertical loss of plastics to the depths is a rapid and dominant process, particularly in areas close to river mouths.

Beaching

In our simulations, to be accurate, we added the *beaching* process– in other words, we consider that if particles leave the *field* where currents have a velocity, they will run aground on the coast or considered on the seabed. The modelling of this process remains a challenge in Lagrangian simulations. Indeed, all the factors – the wind, tides, waves and coastlines structure– to take into account near the coasts are making it hard to predict (Bigdeli et al., 2022; Daily, et al., 2021). Moreover, there is no defined methodology and several ways to compute it in different literature. Because of the variety of approaches, it is also hard to compare the results obtained (Daily et al., 2021). A method found, for example, in Daily et al. (2021) or in the D-WAQ PART model (Bigdeli et al, 2022), and mentioned by Onink et al. (2020) is to calculate beaching with a probability equation. We choose instead to attempt to define it as Castro-Rosero et al. (2023) did, in order to improve the accuracy of our comparisons.

In their study, Onink et al. (2020), test different particle stranding probabilities to simulate beaching. They estimate a beaching rate between 60 and 80%, rising to 90-95% in the north of the basin and on the southern coasts. In our situation, where particles are considered beached as soon as they leave the mask, they have a beaching rate of up to 95% in every scenario. Castro-Rosero et al. (2023) in their study, obtain a different beaching when

they add Stokes Drift in the forces exerted on the particle trajectories. Particles remain for less time, with a mean obtained residence time of 20 days for their scenario with rivers and with higher values, ranging from 50 to 70 days for her homogeneous scenario. While their results were in agreement with those of Stanev and Ricker (2019), this was not the case with the results of Miladinova et al., 2020. The latter obtained beaching after 200 days, on average. While our results for minimum and maximum time to beaching are very similar to those of Castro-Rosero et al. (2023), it is important to note that the addition of sedimentation velocity can have a very marked effect on these dynamics: in our simulations, adding sinking velocity made the proportion of beached particles decrease from 97.58 % to 93.35 %.

As mentioned, it is difficult to compare studies with different methodologies, but despite these different methods, several similarities were found between results (Onink et al., 2020). Note that in the simulations they did, sinking is not taken into account. Nevertheless, their simulations, like ours, have limitations, particularly in coastal areas, where no calculations are added to allow for particle resuspension, anthropogenic cleaning, particle burial or biological ingestion.

Riverine inputs and source distribution

There are differences in the accumulation zones depending on where the particles are initially released. Simulations with particles released from the main rivers accumulate close to the river mouths. As in previous studies of Lagrangian simulations in the Black Sea, particle density is highest in the NW zone, where the Danube, Dnieper and Dniester rivers are located, especially because of the low currents in that part of the basin (Miladinova et al., 2020; Castro-Rosero, L. et al., 2023; Stanev and Ricker, 2019). On the other hand, particles from the scenario with homogeneous release are more evenly distributed, although areas of accumulation are evident at the coasts, as discussed above.

When comparing scenarios 1-3D and 2-80SV, we find that the average travel distance of particles are very similar. This suggests that, beyond a certain sinking rate, horizontal transport remains the dominant factor shaping dispersion. The longest average distances were covered by particles from Yesilirmak, Çoruh and Kizilirmak, with average distances of 436.83 km, 424.59 km and 398.13 km respectively, where in the southeastern quadrant, the mean travelled distances was 359.36. This can be explained by their exposure to stronger currents in this part of the basin, which favor long-range transport (Figure 16). In the southwestern basin, the average travelled distance in the homogeneous scenario is 385.37 km

whereas the distance for particles deployed at the Sakarya river mouth is 385.21 km. This indicates that hydrodynamics in the southwestern basin drives particle transport in a way that is broadly comparable to an idealized uniform input.

Ecological hotspots and environmental risks

In their article, Almpanidou et al. (2021) identify priority conservation areas by applying a risk index, which normalises anthropogenic pressures (e.g., fishing, pollution) and weights them according to their potential impact on biodiversity. This assessment considers a wide range of indicator groups, from zooplankton and bivalve mollusks to crustaceans, pelagic fish, seabirds, and marine mammals (Figure 20). When comparing our results, we find that the accumulation and beaching zones identified in our simulations overlap with areas of species richness (Figure 19). Those areas are defined based on maps from AquaMaps, which combine the number of species with a probability of occurrence above 0.5 within 0.5° grid cell.

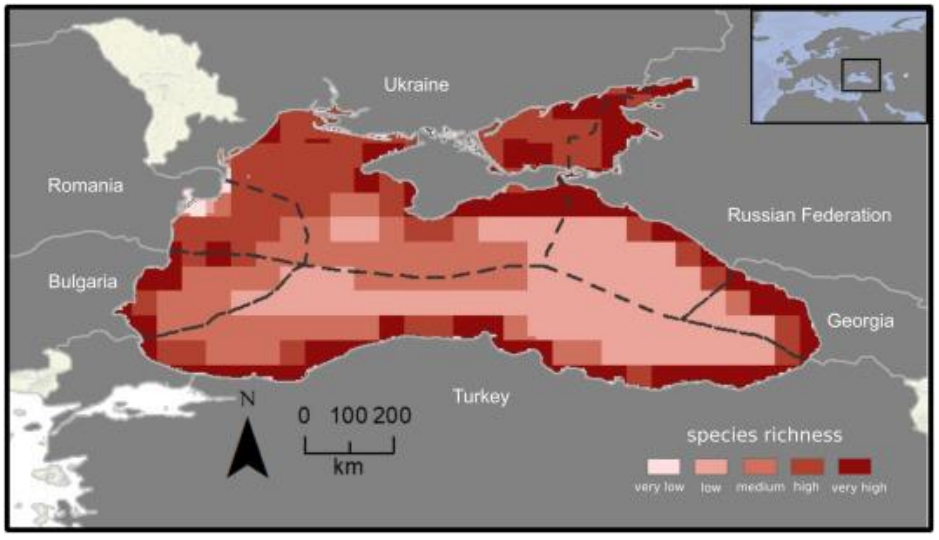

Figure 20 : Species richness in the Black Sea based on the spatial distributions of species from AquaMaps (Kaschner et al., 2019). Exclusive Economic Zones are delineated by black dashed lines (Almpanidou et al., 2021).

In simulations where particles were released from rivers, the northwestern zone is a region where particle density remains relatively high throughout the year. The trajectories also show that, whatever the imposed speed, particles released in this quadrant tend to remain there. This conclusion holds true in the scenario where the initial distribution is homogeneous, as well as in the scenario where river mouths are considered. We can therefore conclude that the NW zone is a very important region to protect, and one in which plastic rate

controls should be seriously considered. This is also the case for particles arriving at the river mouths of Kizilirmak, Yesilirmak and Çoruh, where all particles tend to stay close to the mouth and, thus, accumulate in the “very high species richness” area. In all cases, our 3D simulations have shown that with and without sedimentation velocity, particles beach on the shores of the Black Sea. As shown in Figure 19, all these areas are rich in biodiversity, and it is therefore essential to protect them in all cases.

Methodological limitations and uncertainties

When writing this thesis, it was necessary to make simplification and methodological choices that limit the scope of the work involved in this research.

Firstly, the simulations carried out are based on several simplifying assumptions concerning the properties of plastic particles. They are modeled as spherical, of constant size and density. This is a classic choice when using Ocean Parcel. When using the python library, however, we can impose a diameter and density on the particles, but not their shape. These parameters, as defined earlier in this thesis, are theorized to have a significant impact on the path of microplastic. Particle density depends on the chemical composition of the plastic, and if it ends up being denser than the surrounding density, it will sink. In this thesis, in none of the scenarios do we take these parameters into account, and instead model particle trajectories dropped into the Black Sea.

A second simplification is the failure to take into account degradation, ageing or fragmentation over time. These factors also impact particle density, and should therefore have an impact on their distribution in the pond. Secondly, in the absence of a biofouling module, their density remains fixed, making it impossible to simulate the evolution of their buoyancy - a key factor in the vertical behavior of microplastics (Vladimir et al., 2023). Furthermore, no interaction between particles or with their environment is taken into account: there is no aggregation, collision or mass effect.

Another methodological uncertainty concerns the conversion of inputs in kilotonnes per year into particle numbers. In order to compare our results with previously published work on the Black Sea, we chose to follow the approach of Castro-Rosero et al. (2023), according to which each particle modeled represents a plastic mass of 200 kg. Although this assumption enables the extrapolation of plastic fluxes to the basin scale, it should be understood purely as modelling simplification. Each numerical particle represents a fraction of the total flux, rather than the weight of an actual plastic item, and the choice is not based

on robust local observations. This limitation reflects the lack of systematic and harmonized large-scale studies in the region. Furthermore, the absence of a standardized methodological protocol for counting and quantifying plastic further complicates direct comparison between studies, making it difficult to assess results on a common reference. On the modelling side, one could in principle increase the number of particles to better capture variability, but this is constrained by computational cost.

The numerical schemes used to interpolate velocities and evolve particles (*kernels*) have been based on generic formulations, sometimes poorly adapted to regional specificities or complex plastic properties (shape, density, biofilm, etc.). Incorporating these factors would require more sophisticated parametrisations, for instance by allowing sinking velocities to vary dynamically over time as particles gain or lose buoyancy. Such refinements would substantially increase model complexity and add additional challenges for validation. The advection formula is rewritten by us in the code or simply used from the *Ocean Parcel* library and may therefore be subject to uncertainties and differences from the literature. Another major limitation is the lack of local data on the physical and biological characteristics of microplastics in the Black Sea, which prevents us from fine-tuning the simulated processes.

However, it remains important to note that the principle and purpose of this model is to determine the important factors to be considered in the transport of microplastic particles. It is therefore essential to proceed step by step, without adding everything at once, in order to measure and quantify the impact and uncertainty of each added parameter.

Conclusion and perspectives

In this work, we investigated the transport and fate of microplastics in the Black Sea using Lagrangian simulations. By combining homogeneous and riverine release scenarios, as well as different sinking velocities, we were able to assess both the horizontal and vertical dispersion of particles.

Our results demonstrate that sinking strongly modifies particle dispersion and retention. Slower sinking rates enhance lateral transport in the energetic surface currents, whereas faster sinking rates reduce offshore spreading and lead to stronger retention near river mouths and along the continental slopes. This highlights the importance of incorporating vertical dynamics when evaluating basin-scale transport.

By comparing homogeneous and riverine input scenarios, we showed that riverine sources dominate accumulation patterns, particularly in the northwestern shelf and

southwestern basin, where major river discharge. Unlike the idealized homogeneous scenario, which distributes plastics uniformly, river-based inputs create localized hotspots whose intensity reflects both seasonal discharge variability and bathymetric constraints. These findings emphasize the critical role of land based inputs in shaping spatial heterogenity.

Third, we identified regions most prone to accumulation. Accumulation zones in the 2-6SV and 2-80SV experiments consistently overlapped with areas of ecological sensitivity, such as the northwestern shelf, the Turkish coast, and the northeastern basin. Vertical distribution patterns reflected a balance between surface advection and bathymetric trapping.

To continue this work it would be useful to divide the work into short-term and long-term tasks. Firstly, it would be interesting to investigate more the vertical dynamics in the Black Sea with the sinking speeds. It would be interesting to highlight dynamics such as possible upwelling in the Black Sea (Podymov et al., 2023; Sur et al., 1994) or turbulence in the deeper layers that would provoke the shown oscillations.

In the long term, it would be interesting to model the effect of biofouling. In the marine environment, microplastic particles can be colonized by cultures of bacteria or microalgae, for example. This is known as biofouling. Vladimir et al. (2023) published a study on the vertical and seasonal variations of this process in the Black Sea on PET-type microplastics. They demonstrate that surface particles undergo this colonization at different times and with different intensity, depending on their position in the basin. Some studies (Fischer, R. et al., 2022; Amaral-Zettler, LA., et al., 2021; Lobelle, D. et al., 2021) have investigated how to integrate this process as a *kernel* in Ocean Parcel. Following their methodology to more precisely represent the sinking speed of particles, which has important effects on lateral and vertical transport.

Bibliography

- Aliani, S.; Molcard, A. (2003). Hitch-hiking on floating marine debris: macrobenthic species in the Western Mediterranean Sea, in: Jones, M.B. et al. Migrations and dispersal of marine organisms: Proceedings of the 37th European Marine Biology Symposium held in Reykjavik, Iceland, 5-9 August 2002. Developments in Hydrobiology, 174: pp. 59-67. https://dx.doi.org/10.1007/978-94-017-2276-6_8
- Almpanidou, V., Doxa, A., & Mazaris, A. D. (2021). Combining a cumulative risk index and species distribution data to identify priority areas for marine biodiversity conservation in the Black Sea. Ocean & Coastal Management, 213, 105877. https://doi.org/10.1016/j.ocecoaman.2021.105877
- Alomar, C., & Deudero, S. (2017). Evidence of microplastic ingestion in the shark Galeus melastomus Rafinesque, 1810 in the continental shelf off the western Mediterranean Sea. Environmental pollution, 223, 223-229. https://doi.org/10.1016/j.envpol.2017.01.015
- Amaral-Zettler, L. A., Zettler, E. R., & Mincer, T. J. (2020). Ecology of the plastisphere. Nature Reviews Microbiology, 18(3), 139-151. https://doi.org/10.1038/s41579-019-0308-0
- Amaral-Zettler, L. A., Zettler, E. R., Mincer, T. J., Klaassen, M. A., and Gallager, S. M.: Biofouling impacts on polyethylene density and sinking in coastal waters: A macro/micro tipping point?, Water Res., 201, 117289, https://doi.org/10.1016/j.watres.2021.117289, 2021b.
- Andrady, Anthony L. « Microplastics in the Marine Environment ». Marine Pollution Bulletin, vol. 62, nº 8, août 2011, p. 1596-605. PubMed, https://doi.org/10.1016/j.marpolbul.2011.05.030.
- Andrady, A.L., 2015. Persistence of plastic litter in the oceans. In: Bergmann, M., Gutow, L., Klages, M. (Eds.), Marine Anthropogenic Litter. Springer International Publishing, New York, United States of America, pp. 57–72. https://doi.org/10.1007/978-3-319-16510.
- Atabay, H., Tan, I., Konya, M. Y., Kaman, G., Evcen, A., Çağlayan, H. S., ... & Beken, Ç. P. (2020). Integrated Marine Pollution Monitoring Program: Marine litter studies in the Black Sea coasts of Turkey. Mar. Litter Black Sea, 94-101. https://www.researchgate.net/publication/345292004_Integrated_Marine_Pollution_

Monitoring_Program_Marine_litter_studies_in_the_Black_Sea_coasts_of_Turkey Accessed on the 20.04.2025

- Aytan, U., Esensoy, F. B., Senturk, Y., Arifoğlu, E., Karaoğlu, K., Ceylan, Y., & Valente, A. 2021. Plastic occurrence in commercial fish species of the Black Sea. Turkish Journal of Fisheries and Aquatic Sciences, 22(7). http://doi.org/10.4194/TRJFAS20504
- Aytan, Ü., Esensoy, F. B., Şentürk, Y., Arifoğlu, E., Karaoğlu, K., Ceylan, Y., & Valente, A. (2022). Plastic occurrence in commercial fish species of the Black Sea. doi : http://doi.org/10.4194/TRJFAS20504
- Aytan, U., Kalkan, S., Öztekin, A., Şentürk, Y., Esensoy, F.B. (2019). Concentration and composition of floating marine macro litter in the Southeastern Black Sea. II. National Monitoring of Seas Symposium, Ankara, TURKEY. https://www.researchgate.net/publication/342354287_CONCENTRATION_AND_COMPOSITON_OF_FLOATING_MARINE_MACRO_LITTER_IN_THE_SOUTHEASTERN_BLACK_SEA Accessed on 23.04.2025
- Aytan, U., Senturk, Y., Esensoy, F. B., Oztekin, A., Agırbas, E., & Valente, A. (2020). Microplastic pollution along the southeastern Black Sea. Marine Litter in the Black Sea, 56, 192-207. https://www.researchgate.net/publication/345242036_Microplastic_pollution_along_the_Southeastern_Black_Sea , Accessed on 23.04.2025
- Aytan, U., Valente, A., Senturk, Y., Usta, R., Sahin, F.B.E., Mazlum, R.E., Agirbas, E., 2016. First evaluation of neustonic microplastics in Black Sea waters. Mar. Environ. Res. 119, 22–30. https://doi.org/10.1016/j.marenvres.2016.05.009.
- Bank, M. S., & Hansson, S. V. (2019). The plastic cycle: a novel and holistic paradigm for the Anthropocene. https://pubs.acs.org/doi/10.1021/acs.est.9b02942
- Bakir, A., O'Connor, I.A., Rowland, S.J., Hendriks, A.J., Thompson, R.C., 2016. Relative importance of microplastics as a pathway for the transfer of hydrophobic organic chemicals to marine life. Environ. Pollut. 219, 56–65. https://doi.org/10.1016/j.envpol.2016.09.046
- Barnes, D.K.A., Galgani, F., Thompson, R.C., Barlaz, M., 2009. Accumulation and fragmentation of plastic debris in global environments. Philos. Trans. R. Soc., B 364 (1526), 1985–1998. https://doi.org/10.1098/rstb.2008.0205 .
- Bat, L., Şahin, F., & Öztekin, A. (2018). Current red data list of species in the southern black sea. Discovery Nature, 12, 115-119.

https://www.researchgate.net/publication/328638622_Current_Red_Data_List_of_Species_in_the_Southern_Black_Sea Accessed on 24.03.2025

- Berov, D., & Klayn, S. (2020). Microplastics and floating litter pollution in Bulgarian Black Sea coastal waters. Marine Pollution Bulletin, 156, 111225. DOI: 10.1016/j.marpolbul.2020.111225
- Bigdeli, M., Mohammadian, A., Pilechi, A., & Taheri, M. (2022). Lagrangian modeling of marine microplastics fate and transport: The state of the science. Journal of Marine Science and Engineering, 10(4), 481. https://doi.org/10.3390/jmse10040481
- Bouzaiene, M., Menna, M., Elhmaidi, D., Dilmahamod, A. F., Poulain, P. M. (2021). Spreading of lagrangian particles in the black sea: A comparison between drifters and a high-resolution ocean model. Remote Sensing, 13(13), 2603. https://doi.org/10.3390/rs13132603
- Booth A., Kubowicz S., Beegle-Krause C., Skancke J., Nordam T., Landsem E., Throne-Holst M., Jahren S. (2017). Microplastic in global and Norwegian marine environments: Distributions, degradation mechanisms and transport. Miljødirektoratet, M-918, 1–147. https://www.miljodirektoratet.no/globalassets/publikasjoner/m918/m918.pdf Accessed March 2025.
- Bradney, L., Wijesekara, H., Palansooriya, K. N., Obadamudalige, N., Bolan, N. S., Ok, Y. S., ... & Kirkham, M. B. (2019). Particulate plastics as a vector for toxic trace-element uptake by aquatic and terrestrial organisms and human health risk. Environment international, 131, 104937. https://doi.org/10.1016/j.envint.2019.104937
- Breivik, Ø., Janssen, P. A. E. M., & Bidlot, J.-R. (2016). Approximate Stokes drift profiles in deep water. Ocean Modelling, 100, 49–56. https://doi.org/10.1016/j.ocemod.2016.01.005
- Brennecke, D., Duarte, B., Paiva, F., Caçador, I., Canning-Clode, J., 2016. Microplastics as vector for heavy metal contamination from the marine environment. Estuar. Coast. Shelf Sci. 178, 189–195. https://doi.org/10.1016/j.ecss.2015.12.003 .
- Browne, M.A., Crump, P., Niven, S.J., Teuten, E., Tonkin, A., Galloway, T., Thompson, R. C., 2011. Accumulation of microplastic on shorelines worldwide: sources and sinks. Environ. Sci. Technol. 45 (21), 9175–9179. https://doi.org/10.1021/es201811s .
- BSC. (2007). Marine Litter in the Black Sea Region: A review of the problem.

- Capet, A., Stanev, E. V., Beckers, J. M., Murray, J. W., & Grégoire, M. (2016). Decline of the Black Sea oxygen inventory. Biogeosciences, 13(4), 1287-1297. https://doi.org/10.5194/bg-13-1287-2016
- Castro-Rosero, L. M., Hernandez, I., Alsina, J. M., & Espino, M. (2023). Transport and accumulation of floating marine litter in the Black Sea: insights from numerical modeling. Frontiers in Marine Science, 10, 1213333. https://doi.org/10.3389/fmars.2023.1213333
- Castro-Rosero, L. M., Hernandez, I., Mestres, M., Liste, M., Alsina, J. M., & Espino, M. (2025). Numerical modeling of the dispersion and accumulation of marine litter from the Dniester River in coastal areas of the northwestern Black Sea. Marine pollution bulletin, 213, 117602. https://doi.org/10.1016/j.marpolbul.2025.117602
- Chevalier, S., Beauchard, O., Teacă, A., Begun, T., Todorova, V., Vandenbulcke, L., ... & Grégoire, M. (2025). A macrozoobenthic data set of the Black Sea northwestern shelf. Scientific data, 12(1), 957. https://doi.org/10.1038/s41597-025-05311-2
- Ciliberti S. A., Jansen E., Coppini G., Peneva E., Azevedo D., Causio S., et al. (2022). The black sea physics analysis and forecasting system within the framework of the copernicus marine service. J. Mar. Sci. Eng. 10, 48. doi: 10.3390/jmse10010048
- Cincinelli, A., Scopetani, C., Chelazzi, D., Martellini, T., Pogojeva, M., & Slobodnik, J. (2021). Microplastics in the Black Sea sediments. Science of the Total Environment, 760, 143898. https://doi.org/10.1016/j.scitotenv.2020.143898
- Daily, J., Onink, V., Jongedijk, C. E., Laufkötter, C., & Hoffman, M. J. (2021). Incorporating terrain specific beaching within a lagrangian transport plastics model for Lake Erie. Microplastics and Nanoplastics, 1, 1-13. https://doi.org/10.1186/s43591-021-00019-7
- Desforges, J. P. W., Galbraith, M., Dangerfield, N., & Ross, P. S. (2014). Widespread distribution of microplastics in subsurface seawater in the NE Pacific Ocean. Marine pollution bulletin, 79(1-2), 94-99. https://doi.org/10.1016/j.marpolbul.2013.12.035
- Delandmeter, P. and van Sebille, E. (2019). The Parcels v2.0 Lagrangian framework: new field interpolation schemes, Geosci. Model Dev., 12, 3571–3584, https://doi.org/10.5194/gmd-12-3571-2019 , 2019.
- Delandmeter, P. (2023). PlasticParcels: Lagrangian framework for microplastic simulations [Computer software]. GitHub. https://github.com/OceanParcels/PlasticParcels

- Delandmeter, P., & van Sebille, E. (n.d.). OceanParcels: Lagrangian Ocean Analysis. Retrieved June 30, 2025, from https://docs.oceanparcels.org
- D'Hont, A., Gittenberger, A., Leuven, R. S., & Hendriks, A. J. (2021). Dropping the microbead: Source and sink related microplastic distribution in the Black Sea and Caspian Sea basins. Marine Pollution Bulletin, 173, 112982. https://doi.org/10.1016/j.marpolbul.2021.112982
- Dimassi S. N., Hahladakis J. N., Yahia M. N. D., Ahmad M. I., Sayadi S., Al-Ghouti M. A. (2022). Degradation-fragmentation of marine plastic waste and their environmental implications: A critical review. Arabian Journal of Chemistry, 15, 104262. 10.1016/j.arabjc.2022.104262
- Espenes, H., Carrasco, A., Dagestad, K. F., Christensen, K. H., Drivdal, M., & Isachsen, P. E. (2024). Stokes drift in crossing windsea and swell, and its effect on near-shore particle transport in Lofoten, Northern Norway. Ocean Modelling, 191, 102407. https://doi.org/10.1016/j.ocemod.2024.102407
- Fischer, R., Lobelle, D., Kooi, M., Koelmans, A., Onink, V., Laufkötter, C., Amaral-Zettler, L., Yool, A., and van Sebille, E.: Modelling submerged biofouled microplastics and their vertical trajectories, Biogeosciences, 19, 2211–2234, https://doi.org/10.5194/bg-19-2211-2022 , 2022.
- Frias, J. P., & Nash, R. (2019). Microplastics: Finding a consensus on the definition. Marine pollution bulletin, 138, 145-147. https://doi.org/10.1016/j.marpolbul.2018.11.022
- de la Fuente, R., Drótos, G., Hernández-García, E., López, C., and van Sebille, E.: Sinking microplastics in the water column: simulations in the Mediterranean Sea, Ocean Sci., 17, 431–453, https://doi.org/10.5194/os-17-431-2021 , 2021.
- Galgani, F., Hanke, G., Maes, T., 2015. Global distribution, composition and abundance of marine litter. In: Bergmann, M., Gutow, L., Klages, M. (Eds.), Marine anthropogenic litter. Springer International Publishing, New York, United States of America, pp. 29–56. https://doi.org/10.1007/978-3-319-16510-3 .
- Gewert, B., Plassmann, M. M., & MacLeod, M. (2015). Pathways for degradation of plastic polymers floating in the marine environment. Environmental science: processes & impacts, 17(9), 1513-1521. DOI: 10.1039/C5EM00207A
- Geyer, R., Jambeck, J. R., & Law, K. L. (2017). Production, use, and fate of all plastics ever made. Science advances, 3(7), e1700782. DOI: 10.1126/sciadv.1700782

- González-Fernández, D., Hanke, G., Pogojeva, M., Machitadze, N., Kotelnikova, Y., Tretiak, I., ... & Slobodnik, J. (2022). Floating marine macro litter in the Black Sea: Toward baselines for large scale assessment. Environmental Pollution, 309, 119816. https://doi.org/10.1016/j.envpol.2022.119816
- Goryachkin, Y. N., & Efremova, T. V. (2022). Anthropogenic impact on the lithodynamics of the Black Sea coastal zone of the crimean peninsula. Ecological Safety of Coastal and Shelf Zones of Sea, 1, 6-30. DOI: 10.22 449/2 413 -55 77- 202 2-1 -6- 30
- Grégoire, M., Vandenbulcke, L. and Capet, A. (2020) "Black Sea Biogeochemical Analysis and Forecast (CMEMS Near-Real Time BLACKSEA Biogeochemistry)." Copernicus Monitoring Environment Marine Service (CMEMS). doi: 10.25423/CMCC/BLKSEA_ANALYSISFORECAST_BGC_007_010"
- Gunaalan, K., Almeda, R., Vianello, A., Lorenz, C., Iordachescu, L., Papacharalampos, K., ... & Vollertsen, J. (2024). Does water column stratification influence the vertical distribution of microplastics?. Environmental Pollution, 340, 122865. https://doi.org/10.1016/j.envpol.2023.12286
- Gurielidzei, Z., Kopaliani, N., Devidze, N., Shakaravili M., Javakhishvili, Z. (2012). Black Sea Biodiversity Situation Analysis. Tbilisi, Georgia. https://eiec.gov.ge/En/Documents/Download/1692
- Hautala, S. (2020). *Physics across oceanography: Fluid mechanics and waves*. https://open.umn.edu/opentextbooks/textbooks/physics-across-oceanography-fluid-mechanics-and-waves Accessed on 12.03.2025
- Hersbach, H., Bell, B., Berrisford, P., Biavati, G., Horányi, A., Muñoz Sabater, J., Nicolas, J., Peubey, C., Radu, R., Rozum, I., Schepers, D., Simmons, A., Soci, C., Dee, D., Thépaut, J-N. (2023): ERA5 monthly averaged data on single levels from 1940 to present. Copernicus Climate Change Service (C3S) Climate Data Store (CDS), DOI: 10.24381/cds.f17050d7
- Hidalgo-Ruz, V., Gutow, L., Thompson, R.C., Thiel, M., 2012. Microplastics in the marine environment: a review of the methods used for identification and quantification. Environ. Sci. Technol. 46 (6), 3060–3075. https://doi.org/10.1021/es2031505.
- Ibryamova, S., Toschkova, S., Bachvarova, D. C., Lyatif, A., Stanachkova, E., Ivanov, R., ... & Ignatova-Ivanova, T. (2022). Assessment of the bioaccumulation of

microplastics in the Black Sea mussel Mytilus galloprovincialis L., 1819. J of IMAB, 28(4), 4676-4682. DOI: 10.5272/jimab.2022284.4676

- ISO 472:2013, Plastics - Vocabulary. In International Organization for Standardization: Geneva, 2013. https://www.iso.org/standard/44102.html Accessed on June 2025.
- Ioakeimidis, C., Zeri, C., Kaberi, H., Galatchi, M., Antoniadis, K., Streftaris, N., Galgani, F., Papathanassiou, E., Papatheodorou, G., 2014. A comparative study of marine litter on the seafloor of coastal areas in the eastern Mediterranean and black seas. Mar. Pollut. Bull. 89 (1), 296–304. https://doi.org/10.1016/j.marpolbul.2014.09.044.
- Jalón-Rojas, I., Wang, X.-H., and Fredj, E.: Technical note: On the importance of a three-dimensional approach for modelling the transport of neustic microplastics, Ocean Sci., 15, 717–724, https://doi.org/10.5194/os-15-717-2019 , 2019.
- Jambeck, J. R., Geyer, R., Wilcox, C., Siegler, T. R., Perryman, M., Andrady, A., ... & Law, K. L. (2015). Plastic waste inputs from land into the ocean. science, 347(6223), 768-771. DOI: 10.1126/science.1260352
- Jarosz, E., Teague, W. J., Book, J. W., & Beşiktepe, Ş. (2011). On flow variability in the Bosphorus Strait. Journal of Geophysical Research: Oceans, 116(C8). https://doi.org/10.1029/2010JC006861
- Jørgensen, B. B., Weber, A., & Zopfi, J. (2001). Sulfate reduction and anaerobic methane oxidation in Black Sea sediments. Deep Sea Research Part I: Oceanographic Research Papers, 48(9), 2097-2120. https://doi.org/10.1016/S0967-0637(01)00007-3
- Kaandorp, M. L., Dijkstra, H. A., & van Sebille, E. (2020). Closing the Mediterranean marine floating plastic mass budget: inverse modeling of sources and sinks. Environmental science & technology, 54(19), 11980-11989. https://doi.org/10.1021/acs.est.0c01984
- Kahane-Rapport, S. R., Czapanskiy, M. F., Fahlbusch, J. A., Friedlaender, A. S., Calambokidis, J., Hazen, E. L., ... & Savoca, M. S. (2022). Field measurements reveal exposure risk to microplastic ingestion by filter-feeding megafauna. Nature communications, 13(1), 6327. https://doi.org/10.1038/s41467-022-33334-5
- Kasapoğlu, N., Dağtekin, M., İlhan, S., Erik, G., Özsandikçi, U., & Büyükdeveci, F. (2020). Distribution and composition of seafloor marine litter in the southeastern Black Sea. Marine Litter in, 136.

https://www.researchgate.net/publication/345222822_Distribution_and_composition_of_seafloor_marine_litter_in_the_southeastern_Black_Sea Accessed on 23.04.25

- Kooi, M., Nes, E. H. V., Scheffer, M., & Koelmans, A. A. (2017). Ups and downs in the ocean: effects of biofouling on vertical transport of microplastics. Environmental science & technology, 51(14), 7963-7971. https://doi.org/10.1021/acs.est.6b04702
- Kowalski, N., Reichardt, A. M., & Waniek, J. J. (2016). Sinking rates of microplastics and potential implications of their alteration by physical, biological, and chemical factors. Marine pollution bulletin, 109(1), 310-319. https://doi.org/10.1016/j.marpolbul.2016.05.064
- Krzan, A., Hemjinda, S., Miertus, S., Corti, A., & Chiellini, E. (2006). Standardization and certification in the area of environmentally degradable plastics. Polymer degradation and stability, 91(12), 2819-2833. https://doi.org/10.1016/j.polymdegradstab.2006.04.034
- Lange, M. and van Sebille, E.: Parcels v0.9: prototyping a Lagrangian ocean analysis framework for the petascale age, Geosci. Model Dev., 10, 4175–4186, https://doi.org/10.5194/gmd-10-4175-2017, 2017.
- Laycock, B., Nikolić, M., Colwell, J. M., Gauthier, E., Halley, P., Bottle, S., & George, G. (2017). Lifetime prediction of biodegradable polymers. Progress in Polymer Science, 71, 144-189. https://doi.org/10.1016/j.progpolymsci.2017.02.004
- Lechner, A., Keckeis, H., Lumesberger-Loisl, F., Zens, B., Krusch, R., Tritthart, M., ... & Schludermann, E. (2014). The Danube so colourful: a potpourri of plastic litter outnumbers fish larvae in Europe's second largest river. Environmental pollution, 188, 177-181. https://doi.org/10.1016/j.envpol.2014.02.006
- Li, J., Haeckel, M., Dale, A. W., & Wallmann, K. (2024). Degradation and accumulation of organic matter in euxinic surface sediments. Geochimica et Cosmochimica Acta, 370, 128-143. https://doi.org/10.1016/j.gca.2023.12.030
- Lindeque, P. K., Cole, M., Coppock, R. L., Lewis, C. N., Miller, R. Z., Watts, A. J., ... & Galloway, T. S. (2020). Are we underestimating microplastic abundance in the marine environment? A comparison of microplastic capture with nets of different mesh-size. Environmental Pollution, 265, 114721. https://doi.org/10.1016/j.envpol.2020.114721
- Liubartseva, S., Coppini, G., Lecci, R., & Clementi, E. (2018). Tracking plastics in the Mediterranean: 2D Lagrangian model. Marine pollution bulletin, 129(1), 151-162. https://doi.org/10.1016/j.marpolbul.2018.02.019

- Lobelle, D., Kooi, M., Koelmans, A. A., Laufkötter, C., Jongedijk, C. E., Kehl, C., & van Sebille, E. (2021). Global modeled sinking characteristics of biofouled microplastic. Journal of Geophysical Research: Oceans, 126(4), e2020JC017098. https://doi.org/10.1029/2020JC017098
- Madec, G., and the NEMO team, 2008 : NEMO ocean engine. Note du Pôle de modélisation, Institut Pierre-Simon Laplace (IPSL), France, No 27, ISSN No 1288-1619. https://epic.awi.de/id/eprint/39698/1/NEMO_book_v6039.pdf Accessed on 12.04.2025
- Marcharla E, Vinayagam S, Gnanasekaran L, Soto-Moscoso M, Chen WH, Thanigaivel S, Ganesan S. Microplastics in marine ecosystems: A comprehensive review of biological and ecological implications and its mitigation approach using nanotechnology for the sustainable environment. Environ Res. 2024 Sep 1;256:119181. https://doi.org/10.1016/j.envres.2024.119181
- Markova, N.V. (2023). The Black Sea Deep-Water Circulation: Recent Findings and Prospects for Research. In: Chaplina, T. (eds) Processes in GeoMedia—Volume VI. Springer Geology. Springer, Cham. https://doi.org/10.1007/978-3-031-16575-7_49
- Miladinova, S., Stips, A., Moy, D. M., & Garcia-Gorriz, E. (2020). Pathways and mixing of the north western river waters in the Black Sea. Estuarine, Coastal and Shelf Science, 236, 106630. https://doi.org/10.1016/j.ecss.2020.106630
- Monroy, P., Hernández-García, E., Rossi, V., and López, C.: Modeling the dynamical sinking of biogenic particles in oceanic flow, Nonlin. Processes Geophys., 24, 293–305, https://doi.org/10.5194/npg-24-293-2017, 2017.
- Mukhanov, V. S., Litvinyuk, D. A., Sakhon, E. G., Bagaev, A. V., Veerasingam, S., & Venkatachalapathy, R. (2019). A new method for analyzing microplastic particle size distribution in marine environmental samples. Ecologica Montenegrina, 23, 77-86. https://www.researchgate.net/publication/336406944_A_new_method_for_analyzing_microplastic_particle_size_distribution_in_marine_environmental_samples Accessed on 13.06.2025
- Napper, I. E., Davies, B. F., Clifford, H., Elvin, S., Koldewey, H. J., Mayewski, P. A., ... & Thompson, R. C. (2020). Reaching new heights in plastic pollution—preliminary findings of microplastics on Mount Everest. One Earth, 3(5), 621-630. DOI: 10.1016/j.oneear.2020.10.020
- Nizzetto, L., Futter, M., & Langaas, S. (2016). Are agricultural soils dumps for microplastics of urban origin?.

https://pubs.acs.org/doi/10.1021/acs.est.6b04140#:~:text=https%3A//doi.org/10.1021/acs.est.6b04140

- Nooteboom, P. D., Delandmeter, P., van Sebille, E., Bijl, P. K., Dijkstra, H. A., & von der Heydt, A. S. (2020). Resolution dependency of sinking Lagrangian particles in ocean general circulation models. PloS one, 15(9), e0238650. https://doi.org/10.1371/journal.pone.0238650
- Oguz, T., & Besiktepe, S. (1999). Observations on the Rim Current structure, CIW formation and transport in the western Black Sea. Deep Sea Research Part I: Oceanographic Research Papers, 46(10), 1733-1753. https://doi.org/10.1016/S0967-0637(99)00028-X
- Onink, V., & Laufkötter, C. (2020, April). Modelling the Global Distribution of Beaching. In Proceedings of the 2nd International Conference on Microplastic Pollution in the Mediterranean Sea (p. 299). Springer Nature. Link to ; Accessed on 17.05.2025
- Onink, V., Wichmann, D., Delandmeter, P., & van Sebille, E. (2019). The role of Ekman currents, geostrophy, and stokes drift in the accumulation of floating microplastic. Journal of Geophysical Research: Oceans, 124(3), 1474-1490. https://doi.org/10.1029/2018JC014547
- Oztekin, A., & Bat, L. (2020). Marine litter problem in the southern Black Sea coastal area: An overview of the big pressure in Sinop. Marine litter in the Black Sea, 56, 82-93. https://www.researchgate.net/publication/345135442_Marine_litter_problem_in_the_southern_Black_Sea_coastal_area_An_overview_of_the_big_pressure_in_Sinop Accessed 28.03.2025
- Paiu, A., Mirea, M. C., Gheorghe, A. M., Ionascu, A. S., Paiu, M., Timofte, C., ... & Stefanova, K. (2020). Marine litter monitoring on the Black Sea beaches in 2019: The ANEMONE Project experience. Marine Litter in the Black Sea; Aytan, U., Pogojeva, M., Simeonova, A., Eds, 23-36. https://tudav.org/wp-content/uploads/2020/10/MarineLitterintheBlackSea_tudav.pdf Acessed on 10.03.2025
- Payel, S., Pahlevani, F., Ghose, A., & Sahajwalla, V. (2025). From bulk to bits: understanding the degradation dynamics from plastics to microplastics, geographical influences and analytical approaches. Environmental Toxicology and Chemistry, 44(4), 895-915. https://doi.org/10.1093/etojnl/vgaf037

- Peng, X., Chen, M., Chen, S., Dasgupta, S., Xu, H., Ta, K., ... & Bai, S. (2018). Microplastics contaminate the deepest part of the world's ocean. Geochemical Perspectives Letters, 9(1), 1-5. doi: 10.7185/geochemlet.1829
- Podymov, O. I., Ocherednik, V. V., Silvestrova, K. P., & Zatsepin, A. G. (2023). Upwellings and downwellings caused by mesoscale water dynamics in the coastal zone of Northeastern Black Sea. Journal of Marine Science and Engineering, 11(8), 1628. https://doi.org/10.3390/jmse11081628
- Pojar, I., Stănică, A., Stock, F., Kochleus, C., Schultz, M., & Bradley, C. (2021). Sedimentary microplastic concentrations from the Romanian Danube River to the Black Sea. Scientific reports, 11(1), 2000. https://doi.org/10.1038/s41598-021-81724-4
- Pojar, I., Kochleus, C., Dierkes, G., Ehlers, S. M., Reifferscheid, G., & Stock, F. (2021). Quantitative and qualitative evaluation of plastic particles in surface waters of the Western Black Sea. Environmental Pollution, 268, 115724. https://doi.org/10.1016/j.envpol.2020.115724
- Qiu, Z., Doglioli, A., and Carlotti, F.: Using a Lagrangian model to estimate source regions of particles in sediment traps, Sci.ChinaEarth Sci., 57, 2447–2456, https://doi.org/10.1007/s11430-014- 4880-x , 2014.
- Roullier, F., Berline, L., Guidi, L., Durrieu De Madron, X., Picheral, M., Sciandra, A., Pesant, S., and Stemmann, L.: Particle size distribution and estimated carbon flux across the Arabian Sea oxygen minimum zone, Biogeosciences, 11, 4541–4557, https://doi.org/10.5194/bg-11-4541-2014, 2014.
- Senturk, Y., & Aytan, U. (2024). Microplastic ingestion by planktonic larvae of gastropods and bivalves in the Black Sea. Turkish Journal of Fisheries and Aquatic Sciences, 24(12). DOI : 10.4194/TRJFAS 26829
- Siegel, D., Fields, E., and Buesseler, K. O.: A bottom-up view of the biological pump: Modeling source funnels above ocean sediment traps, Deep-Sea Res. Pt. I, 55, 108–127, 2008. https://doi.org/10.1016/j.dsr.2007.10.006
- Siegel, D. A. and Deuser, W. G.: Trajectories of sinking particles in the Sargasso Sea: modeling of statistical funnels above deepocean sediment traps, Deep-Sea Res. Pt. I, 44, 1519–1541, 1997 https://doi.org/10.1016/S0967-0637(97)00028-9
- Simeonova, A., Chuturkova, R., Toneva, D., & Tsvetkov, M. (2020). Plastic pollution along the Bulgarian Black Sea coast: Current status and trends. Marine Litter in the Black Sea, Turkish Marine Research Foundation (TUDAV), 56, 1-22.

https://www.researchgate.net/publication/345258224_Plastic_pollution_along_the_Bulgarian_Black_Sea_coast_Current_status_and_trends Accessed on 13.03.2025

- Sharma, S., Bhardwaj, A., Thakur, M., & Saini, A. (2024). Understanding microplastic pollution of marine ecosystem: a review. Environmental Science and Pollution Research, 31(29), 41402-41445. https://doi.org/10.1007/s11356-023-28314-1
- Sharma, S., & Chatterjee, S. (2017). Microplastic pollution, a threat to marine ecosystem and human health: a short review. Environmental Science and Pollution Research, 24(27), 21530-21547. https://doi.org/10.1007/s11356-017-9910-8
- Shen, M., Li, Y., Song, B., Zhou, C., Gong, J., & Zeng, G. (2021). Smoked cigarette butts: Unignorable source for environmental microplastic fibers. Science of the Total Environment, 791, 148384. https://doi.org/10.1016/j.scitotenv.2021.148384
- Stanev, E. V. (2005). Black sea dynamics. Oceanography, 18(2), 56-75. https://doi.org/10.5670/oceanog.2005.42
- Stanev, E. V., & Ricker, M. (2019). The fate of marine litter in semi-enclosed seas: a case study of the Black Sea. Frontiers in Marine Science, 6, 660. https://doi.org/10.3389/fmars.2019.00660
- Staneva, J., Ricker, M., & Behrens, A. (2022). Black Sea Waves Reanalysis (CMEMS BS-Waves, EAS4 system) (Version 1) [Data set]. Copernicus Monitoring Environment Marine Service (CMEMS). https://doi.org/10.25423/CMCC/BLKSEA_MULTIYEAR_WAV_007_006_EAS4
- Steer, M., Cole, M., Thompson, R. C., & Lindeque, P. K. (2017). Microplastic ingestion in fish larvae in the western English Channel. Environmental pollution, 226, 250-259. https://doi.org/10.1016/j.envpol.2017.03.062
- Strokal, V., Kuiper, E. J., Bak, M. P., Vriend, P., Wang, M., van Wijnen, J., & Strokal, M. (2022). Future microplastics in the Black Sea: River exports and reduction options for zero pollution. Marine Pollution Bulletin, 178, 113633. https://doi.org/10.1016/j.marpolbul.2022.113633
- Suaria, G., Melinte-Dobrinescu, M.C., Ion, G., and Aliani, S., 2015. First observations on the abundance and composition of floating debris in the North-western Black Sea. Mar. Environ. Res.,107:45-49. http://dx.doi.org/10.1016/j.marenvres.2015.03.011
- Sur, H. İ., Özsoy, E., & Ünlüata, Ü. (1994). Boundary current instabilities, upwelling, shelf mixing and eutrophication processes in the Black Sea. Progress in Oceanography, 33(4), 249-302. https://doi.org/10.1016/0079-6611(94)90020-5

- Thomas, P. J., Perono, G., Tommasi, F., Pagano, G., Oral, R., Burić, P., ... & Lyons, D. M. (2021). Resolving the effects of environmental micro-and nanoplastics exposure in biota: A knowledge gap analysis. Science of the total environment, 780, 146534. https://doi.org/10.1016/j.scitotenv.2021.146534
- Thompson, R. C., Olsen, Y., Mitchell, R. P., Davis, A., Rowland, S. J., John, A. W., ... & Russell, A. E. (2004). Lost at sea: where is all the plastic?. Science, 304(5672), 838-838. DOI: 10.1126/science.1094559
- Topçu, E. N., & Öztürk, B. (2010). Abundance and composition of solid waste materials on the western part of the Turkish Black Sea seabed. Aquatic Ecosystem Health & Management, 13(3), 301-306. https://doi.org/10.1080/14634988.2010.503684
- Toschkova, S., Ibryamova, S., Bachvarova, D. C., Koynova, T., Stanachkova, E., Ivanov, R., ... & Ignatova-Ivanova, T. V. (2024). The assessment of the bioaccumulation of microplastics in key fish species from the Bulgarian aquatory of the Black Sea. BioRisk, 22, 17-31. doi: 10.20944/preprints202308.1799.v1
- van Sebille E, Griffies SM, Abernathey R, Adams TP, Berloff P, Biastoch A, et al. Lagrangian ocean analysis: Fundamentals and practices. Ocean Model. 2018;121(July 2016):49–75. https://doi.org/10.1016/j.ocemod.2017.11.008
- van Sebille, E., Scussolini, P., Durgadoo, J., Peeters, F., Biastoch, A., Weijer, W., Turney, C. S. M., Paris, C. B., and Zahn, R.: Ocean currents generate large footprints in marine palaeoclimate proxies, Nat. Commun., 6, 6521, https://doi.org/10.1038/ncomms7521, 2015. https://doi.org/10.1038/ncomms7521
- Vladimir, M., Tatiana, R., Evgeniy, S., Veerasingam, S., & Bagaev, A. (2023). Vertical and seasonal variations in biofilm formation on plastic substrates in coastal waters of the Black Sea. Chemosphere, 317, 137843. https://doi.org/10.1016/j.chemosphere.2023.137843
- Wei, Xin-Feng, et Mikael S. Hedenqvist. « Heatwaves Hasten Polymer Degradation and Failure ». Science, vol. 381, nº 6662, septembre 2023, p. 1058‑1058. DOI.org (Crossref), https://doi.org/10.1126/science.adj4036.
- Woodall, L. C., Robinson, L. F., Rogers, A. D., Narayanaswamy, B. E., & Paterson, G. L. (2015). Deep-sea litter: a comparison of seamounts, banks and a ridge in the Atlantic and Indian Oceans reveals both environmental and anthropogenic factors impact accumulation and composition. Frontiers in Marine Science, 2, 3. https://doi.org/10.3389/fmars.2015.00003

- Wright, S.L., Thompson, R.C., Galloway, T.S., 2013. The physical impacts of microplastics on marine organism s: a review. Environ. Pollut. 178 (4), 83-492. https://doi.org/10.1016/j.envpol.2013.02.031
- Zambianchi, E., Trani, M., & Falco, P. (2017). Lagrangian transport of marine litter in the Mediterranean Sea. Frontiers in Environmental Science, 5, 5. https://doi.org/10.3389/fenvs.2017.00005
- Zhang, H., 2017. Transport of microplastics in coastal seas. Estuar. Coast. Shelf Sci. 199, 74–86. https://doi.org/10.1016/j.ecss.2017.09.032.
- Zhang F., Zhao Y., Wang D., Yan M., Zhang J., Zhang P., Ding T., Chen L., Chen C. (2021). Current technologies for plastic waste treatment: A review. Journal of Cleaner Production, 282, 124523. 10.1016/j.jclepro.2020.124523 https://doi.org/10.1016/j.jclepro.2020.124523
- Zlateva, I., Ricker, M., Slabakova, V., Slavova, K., Doncheva, V., Staneva, J., ... & Raykov, V. (2024). Analysis of terrestrial and riverine sources of plastic litter contributing to plastic pollution in the Western Black Sea using a lagrangian particle tracking model. Marine Pollution Bulletin, 209, 117108. https://doi.org/10.1016/j.marpolbul.2024.117108

Sites internets :

- International Maritime Organization. (n.d.). Marine litter. Retrieved August 07, 2025, from https://www.imo.org/en/mediacentre/hottopics/pages/marinelitte-default.aspx
- United Nations Environment Programme. (n.d.). Solid waste and marine litter. Retrieved June 10, 2025, from https://www.unep.org/cep/solid-waste-and-marine-litter
- Biotech Academy. (n.d.). The structure of plastic. Retrieved August 21, 2025, from https://www.biotechacademy.dk/en/high-school-projects/plastic-degradation-high-school/the-structure-of-plastic/
- OceanParcels. (n.d.). JIT vs SciPy Particles — Parcels Documentation. Retrieved March 23, 2025, from https://docs.oceanparcels.org/en/latest/examples/tutorial_jit_vs_scipy.html
- PlasticsEurope. (2020). Plastics – the facts 2020. Retrieved April 03, 2025, from https://plasticseurope.org/knowledge-hub/plastics-the-facts-2020/

Annexes

1. Hydrolysis process

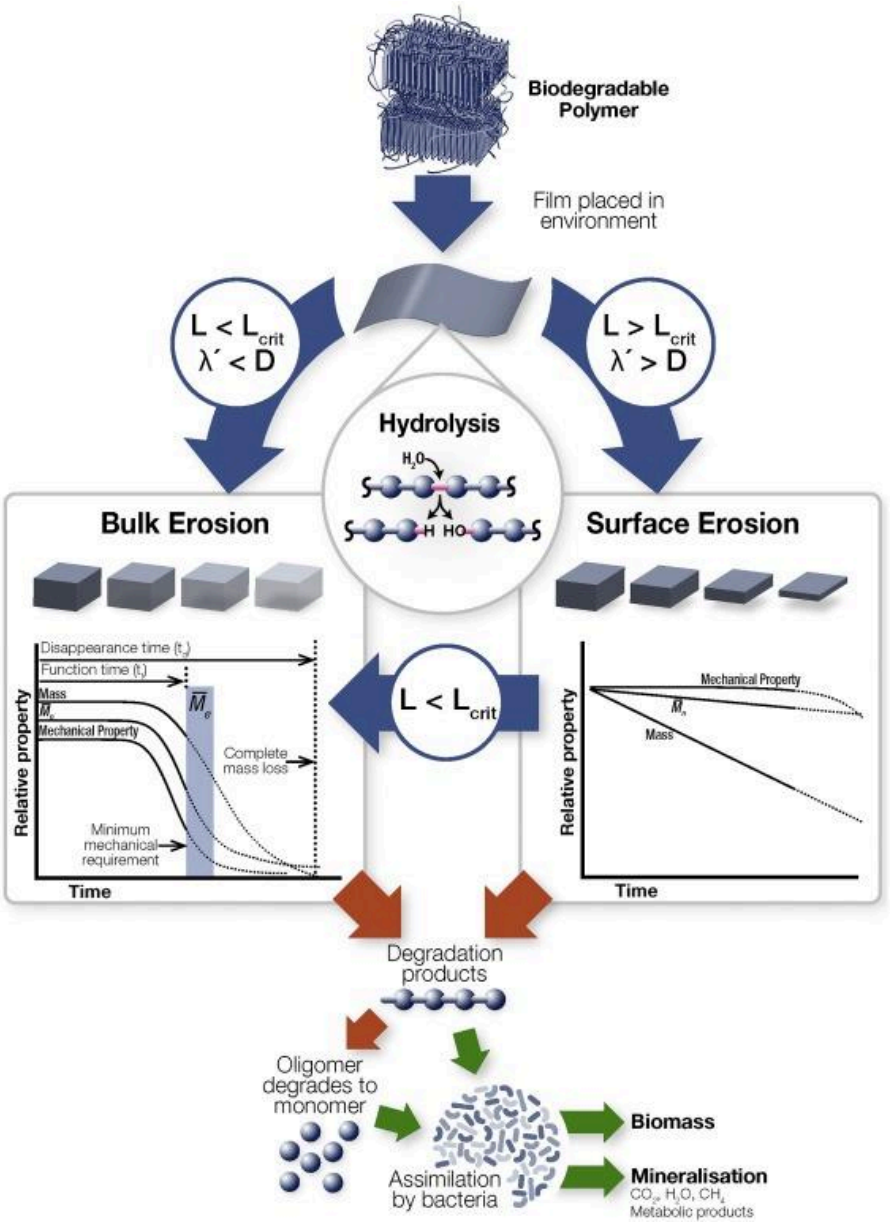

Annex 1 : Steps involved in polymer biodegradation by hydrolysis. The rate of water diffusion into the polymer (*D*) and the pseudo first order rate of hydrolysis (*λ′*). The thickness of the specimen (*L*) and the critical thickness (*Lcrit*) (Laycock et al., 2017)

2. *Depths reached by all particles.*

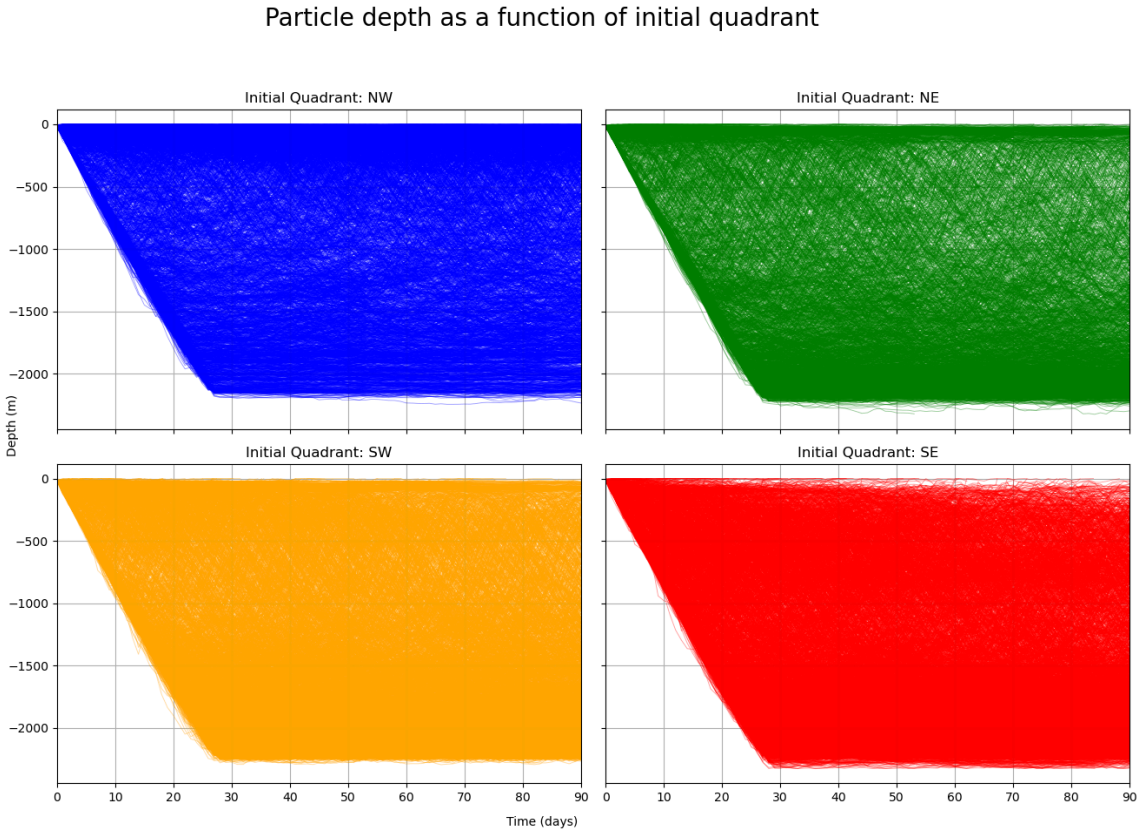

Annex 2 : Depth reached by all particles in the 1-3D scenario. Vertical trajectories of all particles for 90 days.

3. *Depth trajectories of particles released in [44.5°N+, 29°E–33°E]*

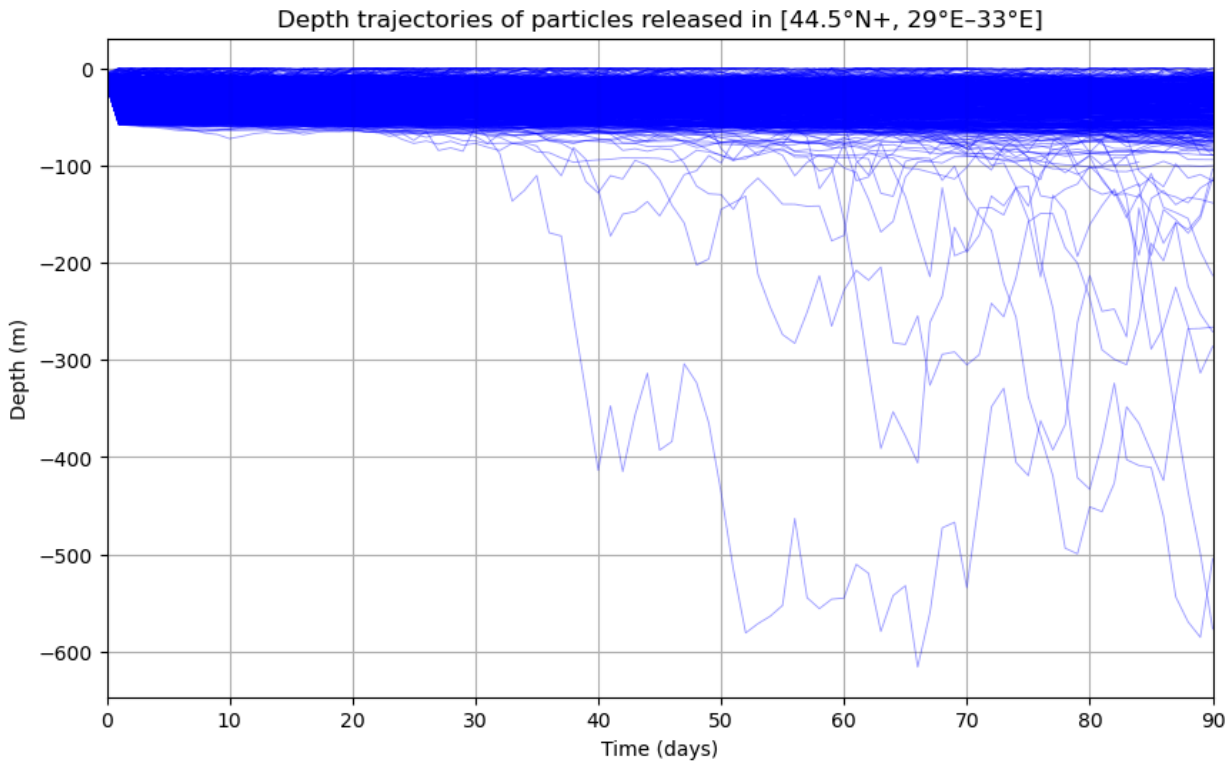

Annex 3 : Depth trajectories of all particles released in the [44.5°N+, 29°E–33°E] within the Black Sea basin.

4. Proportion of particles (%) in the different layers at depth in the Black Sea (2017).

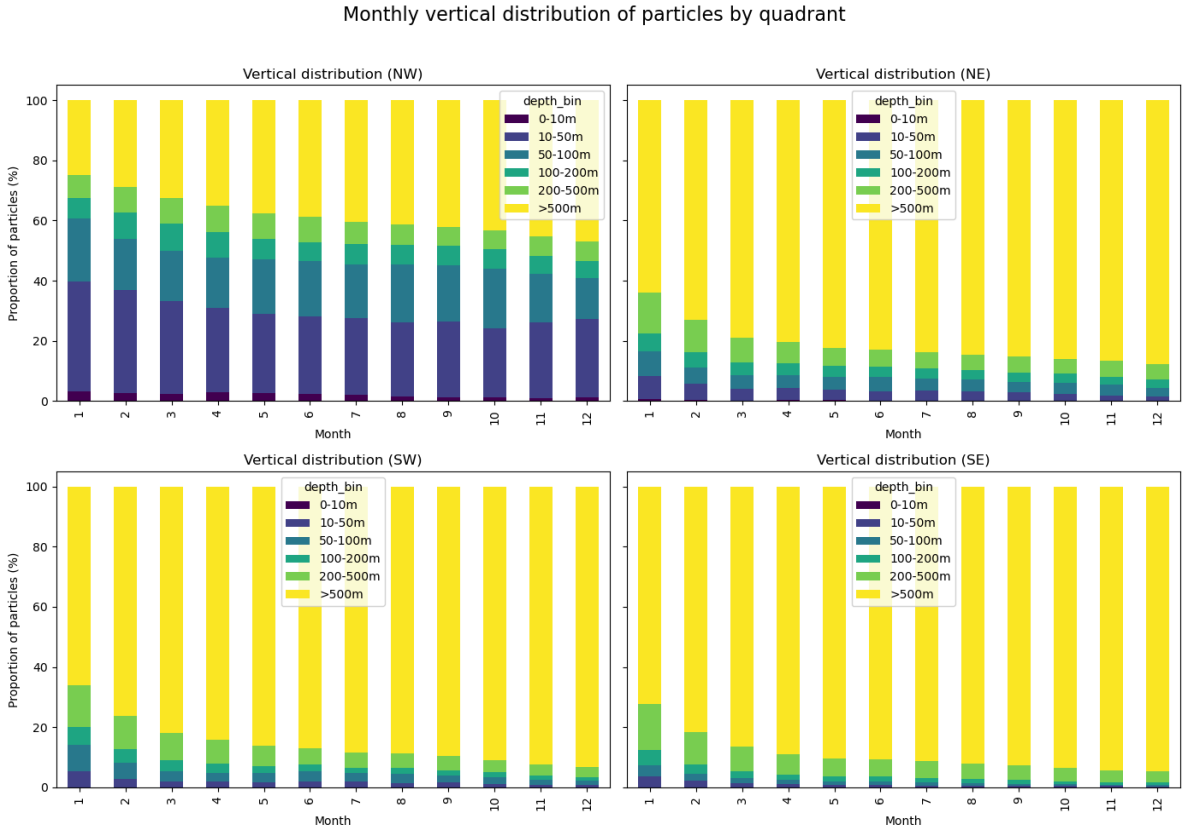

Annex 4 : Proportion of particles (%) in different deplayers at depth in the Black Sea (2017).

5. *Vertical profiles of depth reached by particles in the 2-6SV and 2-80SV*

A : Vertical trajectories of particles with imposed sinking velocity of 6 m/d

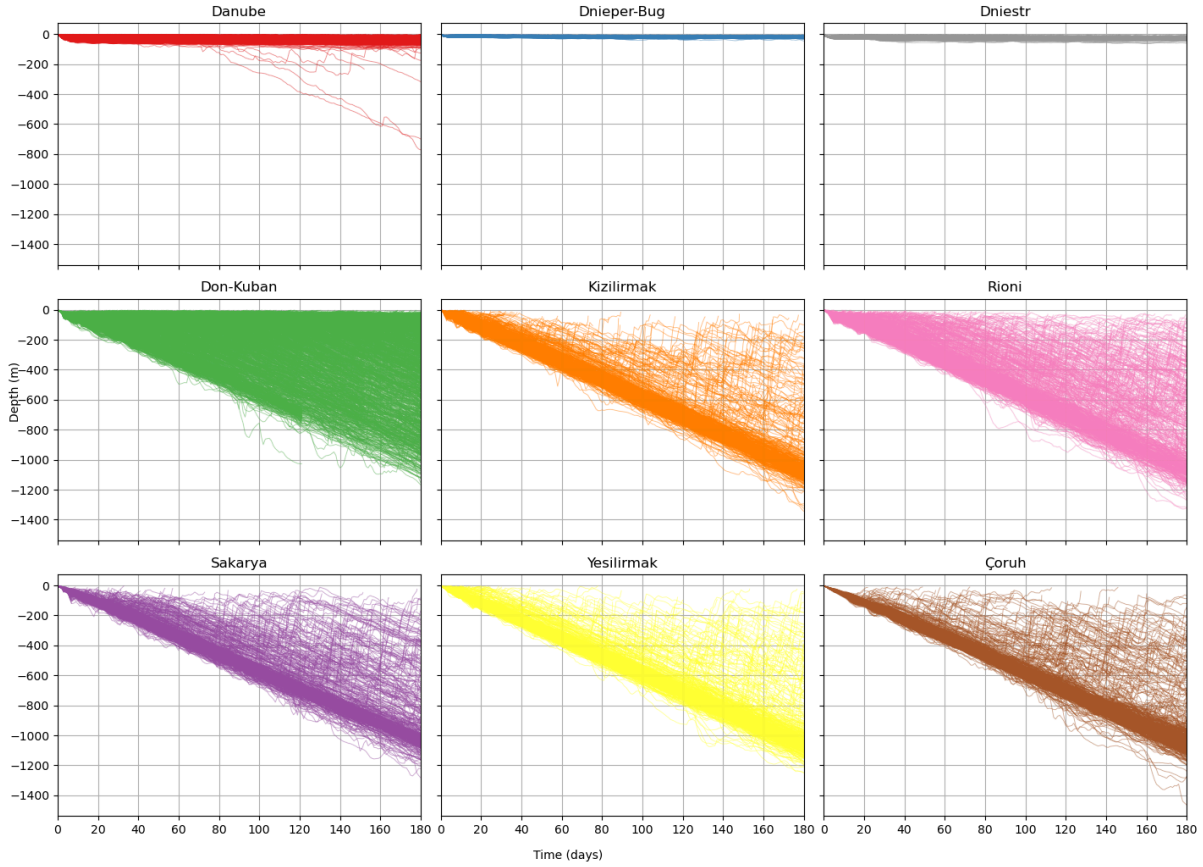

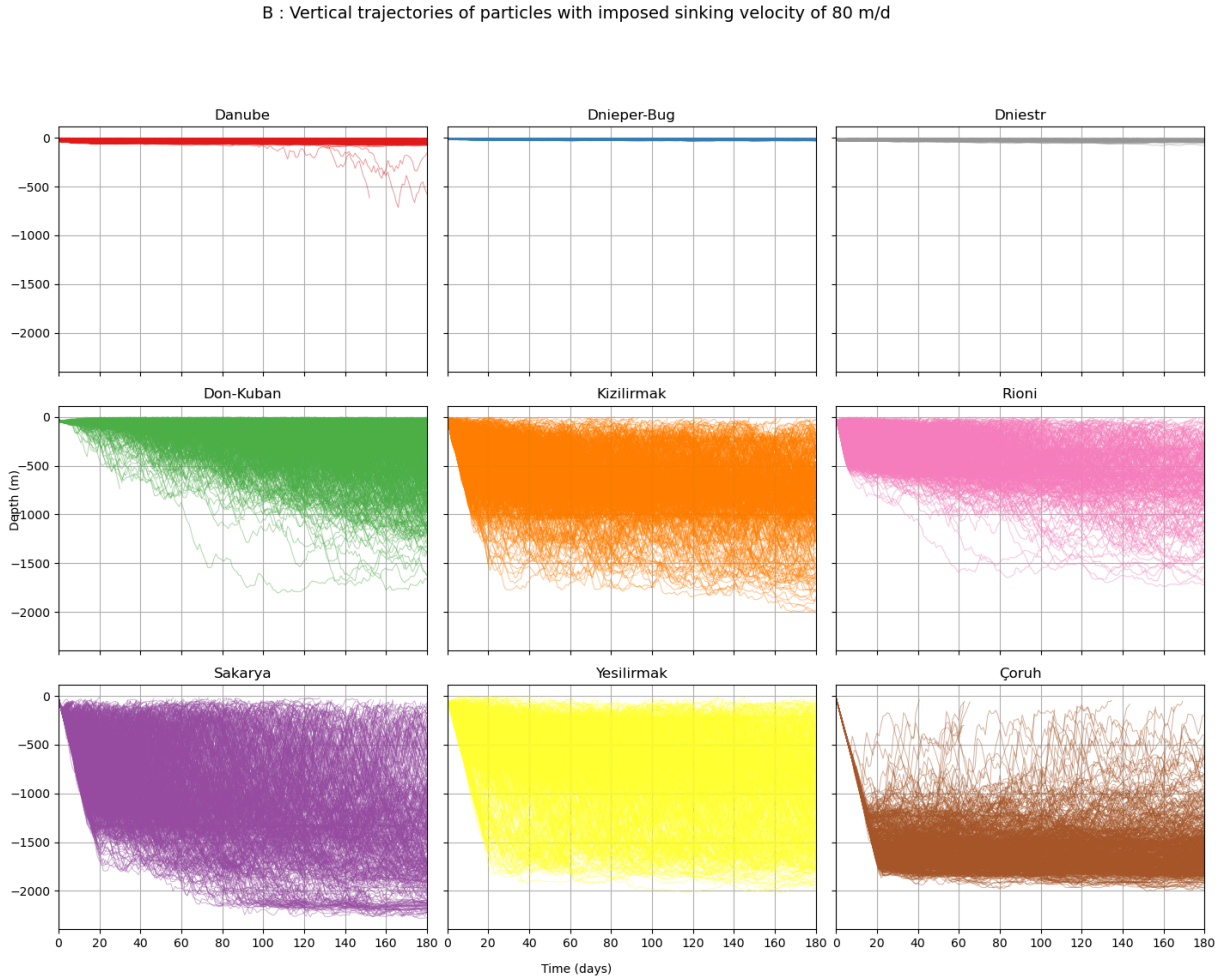

Annex 5 : Depth range reached by the particles in the riverine scenario with an imposed sinking rate of (a) 6m/d, and (b) 80m/day.